EC
Journals.ASM.org

The SrkA Kinase Is Part of the SakA Mitogen-Activated Protein Kinase Interactome and Regulates Stress Responses and Development in *Aspergillus nidulans*

Rafael Jaimes-Arroyo,[a] Fernando Lara-Rojas,[a]* Özgür Bayram,[b] Oliver Valerius,[c] Gerhard H. Braus,[c] Jesús Aguirre[a]

Departamento de Biología Celular y Desarrollo, Instituto de Fisiología Celular, Universidad Nacional Autónoma de México, Mexico City, Mexico[a]; Department of Biology, Maynooth University, National University of Ireland, Maynooth, County Kildare, Ireland[b]; Department of Molecular Microbiology and Genetics, Georg August University, Göttingen, Germany[c]

Fungi and many other eukaryotes use specialized mitogen-activated protein kinases (MAPK) of the Hog1/p38 family to transduce environmental stress signals. In *Aspergillus nidulans*, the MAPK SakA and the transcription factor AtfA are components of a central multiple stress-signaling pathway that also regulates development. Here we characterize SrkA, a putative MAPK-activated protein kinase, as a novel component of this pathway. Δ*srkA* and Δ*sakA* mutants share a derepressed sexual development phenotype. However, Δ*srkA* mutants are not sensitive to oxidative stress, and in fact, *srkA* inactivation partially suppresses the sensitivity of Δ*sakA* mutant conidia to H_2O_2, tert-butyl-hydroperoxide (*t*-BOOH), and menadione. In the absence of stress, SrkA shows physical interaction with nonphosphorylated SakA in the cytosol. We show that H_2O_2 induces a drastic change in mitochondrial morphology consistent with a fission process and the relocalization of SrkA to nuclei and mitochondria, depending on the presence of SakA. SakA-SrkA nuclear interaction is also observed during normal asexual development in dormant spores. Using SakA and SrkA S-tag pulldown and purification studies coupled to mass spectrometry, we found that SakA interacts with SrkA, the stress MAPK MpkC, the PPT1-type phosphatase AN6892, and other proteins involved in cell cycle regulation, DNA damage response, mRNA stability and protein synthesis, mitochondrial function, and other stress-related responses. We propose that oxidative stress induces DNA damage and mitochondrial fission and that SakA and SrkA mediate cell cycle arrest and regulate mitochondrial function during stress. Our results provide new insights into the mechanisms by which SakA and SrkA regulate the remodelling of cell physiology during oxidative stress and development.

We have proposed that when life was confronted with oxidative stress, cells evolved mechanisms not only to defend against reactive oxygen species (ROS) but also to use this ancestral form of stress to regulate their own growth and differentiation (1, 2). Indeed, the regulated production of ROS by enzymes of the NADPH oxidase family (NOX) is essential for sexual differentiation in *Aspergillus nidulans* (3) and *Neurospora crassa* and for polar growth and cell fusion in *N. crassa* (4), and NOX enzymes play multiple signaling functions in other fungal (5–10), animal, and plant species (11). However, little is known about ROS perception and the mechanisms by which ROS exert their signaling functions.

The use of phosphorelay systems to perceive oxidative stress and other types of environmental stress is conserved in bacteria, plants (12), and fungi (13). The fission yeast *Schizosaccharomyces pombe* uses a multistep phosphorelay composed of the Mak2/3 sensor histidine kinases, Mpr1 HPt protein, and Mcs4 response regulator to transmit H_2O_2 stress signals to the Spc1 (also known as StyI) mitogen-activated protein kinase (MAPK) cascade (14, 15). Spc1 is homologous to *Saccharomyces cerevisiae* Hog1 and mammalian p38 MAPKs, which are also involved in stress sensing. Phosphorylated Spc1 phosphorylates the transcription factor Atf1, which mediates most of the transcriptional responses regulated by Spc1, including the induction of many genes involved in the antioxidant response (14). Spc1 also promotes meiosis by inducing the expression of the transcriptional factor Ste11, a regulator involved in sexual development (16). Under osmotic stress, Spc1 interacts with and phosphorylates the Ser/Thr kinase Srk1, which results in a transitory G_2/M cell cycle arrest (17), while Srk1 overexpression inhibits the cell cycle arrest in G_1, under nitrogen starvation. In addition, Srk1 has a regulatory role in meiosis, as null Srk1 mutants enter meiosis earlier than the wild-type strain (18).

In *S. cerevisiae*, the Rck2 kinase, homologous to Srk1, is phosphorylated by Hog1 under oxidative and osmotic stress conditions (19, 20). However, Δ*rck2* mutants are sensitive to oxidative but not to osmotic stress (19), and a deletion of *rck2* suppresses the lethality caused by overactivation of the Hog1 pathway (20). Upon osmotic stress, Rck2 phosphorylates the elongation factor EF2 and transitorily attenuates protein synthesis (20, 21). In the pathogenic fungus *Candida albicans*, Δ*caRck2p* mutants are not sensitive to osmotic stress but show cell wall instability and attenuated virulence in mice (22).

Although filamentous fungi contain homologous stress-sens-

Received 15 December 2014 **Accepted** 20 March 2015

Accepted manuscript posted online 27 March 2015

Citation Jaimes-Arroyo R, Lara-Rojas F, Bayram Ö, Valerius O, Braus GH, Aguirre J. 2015. The SrkA kinase is part of the SakA mitogen-activated protein kinase interactome and regulates stress responses and development in *Aspergillus nidulans*. Eukaryot Cell 14:495–510. doi:10.1128/EC.00277-14.

Address correspondence to Jesús Aguirre, jaguirre@ifc.unam.mx.

* Present address: Fernando Lara-Rojas, Departamento de Microbiología, Division de Biología Experimental y Aplicada, CICESE, Ensenada, Mexico.

Supplemental material for this article may be found at http://dx.doi.org/10.1128/EC.00277-14.

doi:10.1128/EC.00277-14

TABLE 1 *Aspergillus nidulans* strains used in this study

Strain	Genotype	Reference or source
CLK43	*pabaA1 yA2 veA1*	24
FGSCA4	*biA1*	FGSC
TOL1	*pabaA1 yA2* Δ*argB*::*trpC*Δ*B* Δ*sakA*::*argB trpC801 veA1*	24
1155	*pyrG89 pyroA4* Δ*nkuA*::*bar veA1*	Fungal Genetics Stock Center
TRJ1	*pyrG89 pyroA4 srkA*::*GFP* Δ*nkuA*::*bar veA1*	This work; 1155 transformed with PCR construct srkA-gfp-AfpyrG
TRJ2	*pyrG89 pyroA4 srkA*::*s-tag*::*AfpyrG* Δ*nkuA*::*bar veA1*	This work; 1155 transformed with PCR construct srkA-s-tag-AfpyrG
TRJ4	*pyrG89 pyroA4* Δ*srkA*::*afpyrG* Δ*nkuA*::*bar veA1*	This work; 1155 transformed with PCR construct ΔsrkA-AfpyrG
TRJ5	*pyrG89 pyroA4 srkA*::*GFP bio*::*pyroA*::*gpdA*::*h2A*::*mrfp*::*bio* Δ*nkuA*::*bar veA1*	This work; TRJ1 transformed with construct bio-pyroA-gpdA-h2A-mrfp-bio
TRJ6	*pabaA1 yA2* Δ*argB*::*trpC*Δ*B* Δ*sakA*::*argB srkA*::*GFP ph2A*::*h2A*::*mrfp-ptrA trpC801 veA1*	This work; CRJ3 transformed with the construct ph2-h2A-mrfp-ptrA
TRJ7	*pyrG89 pyroA4 bio*::*pyroA*::*gpdA*::*h2A*::*mrfp*::*bio* Δ*nkuA*::*bar veA1*	This work; 1155 transformed with construct bio-pyroA-gpdA-h2A-mrfp-bio
CRJ2	*pabaA1 yA2* Δ*srkA*::*AfpyrG veA1*	This work; progeny from TRJ4 × CLK43
CRJ3	*pabaA1 yA2* Δ*argB*::*trpC*Δ*B* Δ*sakA*::*argB srkA*::*gfp trpC801 veA1*	This work; progeny from TRJ1 × TOL1
CRJ5	*pabaA1 yA2* Δ*sakA*::*argB* Δ*srkA*::*AfpyrG veA1*	This work; progeny from TOL1 × TRJ4
TFL22	*pyrG89 pyroA4 sakA*::*s-tag*::*AfpyrG* Δ*nkuA*::*bar veA1*	This work; 1155 transformed with PCR construct sakA-s-tag-AfpyrG
CRJ6	*pabaA1 yA2* Δ*sakA*::*argB*	This work; progeny from TOL1 × FGSCA4
CRJ7	*pabaA1 yA2* Δ*srkA*::*AfpyrG*	This work; progeny from CRJ2 × FGSCA4
CRJ8	*pabaA1 yA2* Δ*sakA*::*argB* Δ*srkA*::*AfpyrG*	This work; progeny from CRJ5 × FGSCA4
CRJ9	*pabaA1 yA2*	This work; progeny from CLK43 × FGSCA4

ing proteins, these appear to be adapted in specific ways in different fungi, according to the niche and biology of every species. The *A. nidulans* Spc1 orthologous MAPK SakA is activated by a conserved phosphorelay system (23), in response to osmotic, oxidative, and nutrient starvation stress (24, 25), as well as during asexual development (24). SakA interacts with the b-Zip transcription factor AtfA, which activates the catalase genes *catA* and *catB* during oxidative stress (25) and both Δ*sakA* and Δ*atfA* mutants are sensitive to oxidative stress. SakA was also identified as HogA (26) and together with AtfA was shown to be involved in gene regulation in response to osmotic stress (27). In many other filamentous fungi, SakA orthologs have been found to be involved in osmotic and/or oxidative-stress resistance and the regulation of development and/or pathogenicity (28–32). *A. nidulans sakA*-null mutants also show premature sexual development and produce asexual spores (conidia) that progressively lose their viability (24, 25). Indeed, SakA accumulates in conidia in an AtfA-dependent way, is phosphorylated during conidium development, and requires dephosphorylation for germination. Therefore, SakA phosphorylation regulates the transition between latency (spore) and growth (germination), in a process that is conserved in other fungi (25).

As not all the mechanisms by which SakA phosphorylation regulates stress responses, sexual development, and spore functions are known, this work was aimed at identifying other SakA targets that could mediate these and other SakA functions. We report that SrkA, a member of the CAMK (Ca^{2+}/calmodulin-dependent kinase) family, is a novel component of the SakA stress MAPK pathway and identify potentially new protein targets for both kinases. We demonstrate that SakA and SrkA show functional and physical interactions and that the SakA-SrkA pathway plays differential roles in the antioxidant response and development. Furthermore, we show that H_2O_2 induces mitochondrial fragmentation, consistent with a fission process and the relocalization of SakA to nuclei and mitochondria, depending on the presence of SakA.

MATERIALS AND METHODS

Strains, media, and growth conditions. *A. nidulans* strains used in this work are listed in Table 1. All strains were grown at 37°C in 1% glucose minimal medium containing nitrate as the nitrogen source (33) and needed supplements. For oxidative-stress sensitivity experiments, H_2O_2, tert-butyl-hydroperoxide (*t*-BOOH), menadione, paraquat, and methylglyoxal were filter sterilized and added to agar medium before solidification. Δ*sakA*, Δ*srkA*, and Δ*sakA* Δ*srkA* strains in a *veA*$^+$ background were obtained from sexual crosses with strain FGSCA4 (Table 1). The presence of the *veA*$^+$ allele was confirmed by PCR using genomic DNA from selected progeny and the primers *veA*$^+$ forward and *veA*$^+$ reverse, as reported elsewhere (34). For sexual induction, 1×10^5 conidia were homogeneously inoculated onto plates containing 2% glucose agar minimal medium, and plates were sealed with masking tape and incubated at 37°C. The number of cleistothecia per square centimeter was determined as previously described (24).

Deletion of the *srkA* gene and tagging of SakA and SrkA. A cassette for *srkA* gene deletion was obtained by double joint PCR (35). 5′ and 3′ *srkA* fragments were amplified with primers 5′SrkAFor-5′SrkARev+tail and 3′SrkAFor+tail-3′SrkARev, respectively (see Table 2 for primer sequences). The *A. fumigatus pyrG* marker was amplified from plasmid PFNO3 with primers pyrGforward and pyrGreverse (36). These three fragments were used in a fusion PCR with primers 5′Nest AN4483 and 3′Nest AN4483. The final 4,600-bp 5′SrkA-AfpyrG-3′SrkA product was purified and used to transform *A. nidulans* Δ*nkuA* strain 1155 by protoplast fusion (37). Twenty *pyrG*$^+$ transformants were obtained, and 10 were analyzed by PCR-restriction analyses to confirm the elimination of *srkA*. Strain TRJ4 was chosen for further analysis and crossed with strain CLK43 to get rid of the Δ*nkuA* mutation. Strain CRJ2 was confirmed by PCR-restriction analysis and used in further experiments (see Fig. S2 in the supplemental material). A similar strategy was used to generate SrkA::GFP, SrkA::S-tag, and SakA::S-tag constructs. For the SrkA C-terminal GFP construct (38), 5′ and 3′ PCR fragments were obtained with primers GSP1AN4483-GSP2AN4483 and GSP3AN4484-GSP4AN4483, respectively. The *A. fumigatus pyrG* cassette was amplified with primers GFP1AN4483-GFP2AN4483, using plasmid PFNO3 as the template. The final PCR product was obtained with primers AN4483NES1 and AN4483NES2 and the resulting 6,747-bp

TABLE 2 DNA primers used in this study

Primer	Sequence 5′ to 3′
5′SrkA For	TCGCAGCCGAAGGAGTCAAG
5′SrkARev+tail	GGTGAAGAGCATTGTTTGAGG CTGTGCTCATGGTAGGAAAGG
3′SrkAFor+tail	GCATCAGTGCCTCCTCTCAGACGGGCCATTCTCTTCTCAATC
3′SrkA Rev	AGCGGCCGTCTTCTGTCTCG
5 Nest AN4483	GTTGGACGACAGCAACGG
3 Nest AN4483	TTTAAGCGAACGAGCACG
AN4483 GSP1	ATTGCCTTGCCTCCTCGACCTTTTCC
AN4483 GSP2	CATGGCAGGCTGCTCTTGATGTCTTC
AN4483 GSP3	GCGTCTCTACGACTTGATTAGGGTTC
AN4483 GSP4	TTCAGTTGAAACCGTTCATCATGACC
AN4483 GFP1	AGAAGACATCAAGAGCAGCCTGCCATGGGAGCTGGTGCAGGCGCTGGAGC
AN4483 GFP2	GTGAACCCTAATCAAGTCGTAGAGACGCGTCTGAGAGGAGGCACTGATGC
AN4483NES1	CCTCCCTTTCCTACCATGAG
AN4483NES2	TACCGCAATTACGCCATTAC
GSP1sakA	GCCTGCCCAAGTGCGTGCGGTCTATT
GSP2sakA	TTGGAAACCTTGCTGGTTGAGCCCGGCTCC
GSP3sakA	AGCCCTAATGAATCGCGTGGATGCGGCGCT
GSP4sakA	CATGCATAGCCGTTCGCATCTTGAGCCG
GFP1sakA	GGAGCCGGGCTCAACCAGCAAGGTTTCCAAGGAGCTGGTGCAGGCGCTGGAGCCGGTGCC
GFP2sakA	AGCGCCGCATCCACGCGATTCATTAGGGCTGTCTGAGAGGAGGCACTGATGC
5′Nest-sakA	TGGAGCGGTAAAGCGTCC
3′Nest-sakA	TCAGCAAGCATCCCAAGG
pyrGforward	GCCTCAAACAATGCTCTTCACC
pyrGreverse	GTCTGAGAGGAGGCACTGATGC
veA^+ forward	TGTGTTATCCCATCAAGAGG
veA^+ reverse	TCTCCGCGCCGTCTCATC

srkA-GFP-AfpyrG fragment was used to transform strain 1155. Plasmid pHL81 (39), containing the S-tag sequence, was used to obtain the SrkA::S-tag replacement cassette. 5′ and 3′ fragments were amplified with primers GSP1AN483-GSP2AN4483 and GSP3AN4483-GSPAN4483, respectively. S-tag and *A. fumigatus pyrG* fragments were amplified with primers GFP1AN4483 and GFP2AN4483. A 6,657-bp fusion PCR product obtained with primers AN4483NES1 and AN4483NES2 was used to transform strain 1155. For the SakA::S-tag construct, 5′ and 3′ fragments were amplified with primers GSP1sakA-GSP2sakA and GSP3sakA-GSPsakA4, respectively, and the S-tag sequence was amplified with primers GFP1sakA and GFP2sakA. The 5,728-bp fusion PCR product obtained with primers 5NestSakA-GFP and 3′Nest-sakA was used to transform strain 1155. To label nuclei, transformants containing the SrkA::GFP construct were retransformed with the H2A::mRFP (monomeric red fluorescent protein) fragment bio-left-ORF-pyroA-gpdA-h2A-mrfp-bio-right-ORF, derived from plasmid pOB340 (40). The SrkA::GFP/Δ*sakA* strain CRJ3, obtained as progeny from a cross between strains TRJ1 and TOL1, was transformed with the fragment ph2A::h2A::mrfp-ptrA, obtained from plasmid pON307 (40).

Microscopy. Fluorescence microscopy images were captured *in vivo*. Spores from GFP-containing strains were grown for 12 h in an 8-well borosilicate cover glass system (Nunc) containing liquid minimal medium at 37°C and no shaking. After this, some samples were shifted to the same medium containing 30 mM H_2O_2 and incubated for 30 min. For mitochondrial-fragmentation experiments, conidia were streaked for single colonies and grown for 12 h at 37°C. After this, agar blocks containing single colonies were cut out from the plates, covered with MitoTracker red for 2 min (Invitrogen, Carlsbad, CA) as reported elsewhere (41), transferred to small petri plates, and submerged in water with or without 30 mM H_2O_2. At different times, hyphae from the growing edge of the colonies were observed and photographed using fluorescence microscopy. Photographs were taken using a Zeiss Axiovert Observer Z1 microscope or a Nikon Eclipse E600 epifluorescence microscope, connected to a Neo Andor sCMOS cooled camera.

S-tag protein purification and identification by LC-MS/MS. To precipitate S-tag-labeled proteins, protein crude extracts were prepared from cultures incubated with or without H_2O_2, as follows. A total of 2.5×10^6 spores were used to inoculate 200 ml of liquid culture and incubated for 12 h at 37°C, with shaking. After this, the culture was treated with 10 mM H_2O_2 for 10 min or left untreated. Protein purification was performed as reported previously (40). Briefly, samples were frozen with liquid nitrogen, ground, and resuspended in 5 ml of protein extraction buffer (50 mM Tris [pH 7.5], 100 mM KCl, 10 mM $MgCl_2$, 0.1% NP-40, 10% glycerol, 20 mM *b*-glycerophosphate, 2 mM Na_3VO_4, 5 mM NaF, 0.5 mM phenylmethylsulfonyl fluoride [PMSF], 1 mM benzamidine, 1 mM EGTA, 1 mM dithiothreitol [DTT], and 2× protease inhibitors [Roche]). After two centrifugation steps at 4°C, the supernatant was transferred to a new tube and incubated at 4°C with 300 μl of S-protein agarose slurry (Novagen) per 100 mg of protein in a rotary shaker for 2 h. After this, S-protein beads were collected by centrifugation and the supernatant was discarded. Beads were washed twice and resuspended in 1 ml of protein extraction buffer. Protein extraction was performed twice using 1 ml of extraction buffer. Purified supernatant was incubated with 50 μl of 3× Laemmli gel loading dye, boiled at 95°C for 10 min, and stored at −80°C until used. Liquid chromatography-tandem mass spectrometry (LC-MS/MS) protein identification was done as described by Bayram et al. (42).

Immunoblot detection. A total of 2.5×10^6 spores were used to inoculate 200 ml of liquid medium and incubated at 37°C with shaking for 12 h. After this, mycelium was filtered, rinsed with distilled water, frozen with liquid nitrogen, and ground with a mortar. Mycelial powder was resuspended in protein extraction buffer (see above) and used as total crude extract or processed for protein purification (see above). Thirty micrograms of protein was used for immunoblotting as reported elsewhere (24), using anti-Hog1 (y-215) polyclonal (Santa Cruz Biotechnology), anti-phospho-p38 MAP kinase (Cell Signaling Technology), and anti-S-tag (ICL Laboratories) antibodies. Horseradish peroxidase (HRP)-conjugated secondary antibodies (Zymed Laboratories) and Pierce Super-

Signal chemiluminescent substrate (Thermo Scientific) were used for detection.

RESULTS

The elimination of the *srkA* gene does not result in oxidative-stress sensitivity, and its inactivation partially suppresses oxidative-stress sensitivity of Δ*sakA* conidia. As a strategy to detect other components of the SakA MAPK pathway in filamentous fungi, we focused on the *A. nidulans* gene AN4483, encoding a homolog of *S. pombe* Srk1 MAPK-activated protein kinase, which acts downstream of the SakA ortholog StyI/Spc1 (18). AN4483 encodes a 611-amino-acid protein that shows 59% identity to Srk1 and 49% identity to *S. cerevisiae* Rck2. A protein alignment of AN4483 with other members of the CAMK (Ca^{2+}/calmodulin-dependent kinase) family, including *C. albicans* CaRck2 and proteins from *N. crassa* and from other aspergilli is shown in Fig. S1 in the supplemental material. All these proteins contain a kinase-regulatory domain, with a glycine-rich sequence not found in any other kinases (43), as well as a putative MAPK-binding site near the C terminus. In addition, we determined that AN4483 and the homologs from filamentous fungi contain a highly conserved N-terminal putative mitochondrial targeting sequence (see Fig. S1 in the supplemental material). A recent publication identified the AN4483 gene as *cmkD* and reported that its deletion did not produce any obvious phenotype (44). Here, we propose renaming the *A. nidulans* AN4483 protein SrkA, based on the fact that *S. pombe* Srk1 is the best-characterized ortholog of this family. In assessing SrkA function, we first deleted the *srkA* gene by homologous recombination gene replacement. We transformed the *nkuA*-lacking strain 1155 using a double-joint PCR strategy and the *A. fumigatus pyrG* gene as a selective marker (see Fig. S2A in the supplemental material). Ten $pyrG^+$ transformants, out of 20 transformants obtained, were subjected to PCR and restriction analysis to confirm *srkA* elimination (see Fig. S2B in the supplemental material), and Δ*srkA* strain 26 was renamed TRJ4 and chosen for further characterization. The most evident phenotype in all Δ*srkA* strains was the production of high numbers of Hülle cells and a derepression of sexual development (see Fig. 2; also, see Fig. S3 and S6 in the supplemental material). When strain TRJ4 was crossed to strain CLK43, the linkage between this phenotype and the *pyrG* marker was confirmed. Furthermore, the deletion of the *srkA* gene using the *A. fumigatus pyroA* gene also produced a sexual-derepression phenotype that was linked to this marker (data not shown).

As a first step to determine if SrkA acted downstream of SakA, we compared the sensitivities of Δ*sakA* and Δ*srkA* single and double mutants to different types of stress. We found that in contrast to Δ*sakA* strains, Δ*srkA* mutants were not sensitive to the cell wall-stressing compound calcofluor (see Fig. S4 in the supplemental material). Likewise, Δ*sakA* but not Δ*srkA* mutants were partially resistant to the fungicide fludioxonil (see Fig. S5 in the supplemental material), which induces constitutive activation of SakA (25). These results indicate that the potential role of SrkA as a downstream component of the SakA pathway does not involve the regulation of cell wall integrity or fludioxonil sensitivity.

As SakA regulates antioxidant responses through the transcription factor AtfA (25) and Δ*sakA* and Δ*atfA* mutants are both sensitive to oxidative stress, we evaluated SrkA function during oxidative stress. For this, we grew spores and mycelia from Δ*sakA* and Δ*srkA* single and double mutants in the presence of H_2O_2, the organic peroxide tert-butyl-hydroperoxide (*t*-BOOH), menadione, paraquat (Fig. 1), and methylglyoxal (not shown). As shown in Fig. 1A, Δ*sakA* mutant conidia were sensitive to the oxidative-stress-causing agents H_2O_2, *t*-BOOH, and menadione, while Δ*sakA* mutant mycelia were more sensitive only to *t*-BOOH (Fig. 1B). In contrast, Δ*srkA* conidia displayed a pattern of resistance to all these compounds that was similar to the one shown by the wild-type strain. Unexpectedly, conidia from Δ*sakA* Δ*srkA* mutants showed higher resistance to H_2O_2 (4.5 mM), *t*-BOOH (0.5 mM), and menadione (60 μM) than the Δ*sakA* single mutant (Fig. 1A). Mycelia from single and double mutants showed similar patterns of resistance to these compounds, except that the Δ*sakA* Δ*srkA* mutant displayed decreased resistance to 0.5 mM *t*-BOOH. These results indicate that the MAPK SakA and the CAM kinase SrkA play antagonistic roles in the response of conidia to the oxidative stress caused by H_2O_2, *t*-BOOH, and menadione.

SrkA represses sexual development independently of SakA. The SakA MAPK not only regulates stress responses but also represses sexual development (24, 25). To determine if SrkA mediated this repression, we followed sexual development of Δ*sakA* and Δ*srkA* single and double mutants and determined the number of fruiting bodies or cleistothecia. Results in Fig. 2 show that, as reported before (24), a Δ*sakA* mutant produces higher numbers of cleistothecia than a wild-type (WT) strain. The Δ*srkA* strain also developed more cleistothecia than the WT strain but not as many as the Δ*sakA* mutant. Notably, the Δ*sakA* Δ*srkA* strain showed an additive phenotype, forming about 7 times more cleistothecia than the WT strain after 7 days of induction of sexual development.

The *A. nidulans veA* gene encodes a member of a protein family conserved in fungi which is required for cleistothecium formation (45) and regulation of secondary metabolism (42). As our laboratory strains contain a *veA1* allele that results in higher production of conidia and lower numbers of cleistothecia (46), we also evaluated the Δ*sakA* and Δ*srkA* sexual-derepression phenotypes in the presence of a wild-type *veA* allele. Results in Fig. S3 in the supplemental material show that in the veA^+ background, all strains produced much higher numbers of cleistothecia than equivalent *veA1* strains after 5 days of induction (Fig. 2). As before, Δ*sakA* and Δ*srkA* mutants showed sexual-derepression phenotypes. In this case, the double mutant did not show an additive phenotype in the production of cleistothecia. However, there was a massive production of Hülle cells, suggesting that many structures initiate sexual development but some fail to complete the process and that SrkA repression of sexual development also occurs in a veA^+ background. These and the oxidative-stress sensitivity results (Fig. 1) indicate that SakA and SrkA regulate both the antioxidant response and sexual development and suggest antagonistic and non-antagonistic SakA-SrkA interactions during these two processes, respectively.

H_2O_2 induces mitochondrial fragmentation and a relocalization of SrkA that depends on the presence of SakA. In response to stress, SakA is phosphorylated and accumulates in the nucleus (25). To further explore SakA-SrkA interactions, we determined SrkA localization with and without oxidative stress. For this purpose, we generated strains in which *srkA* was replaced by a functional (see Fig. S6 in the supplemental material) *srkA*::*GFP* allele, in WT and Δ*sakA* genetic backgrounds. In addition, a H2A::RFP construction was introduced in these strains, as a nuclear marker. Results in Fig. 3 show that without H_2O_2, SrkA::GFP was excluded

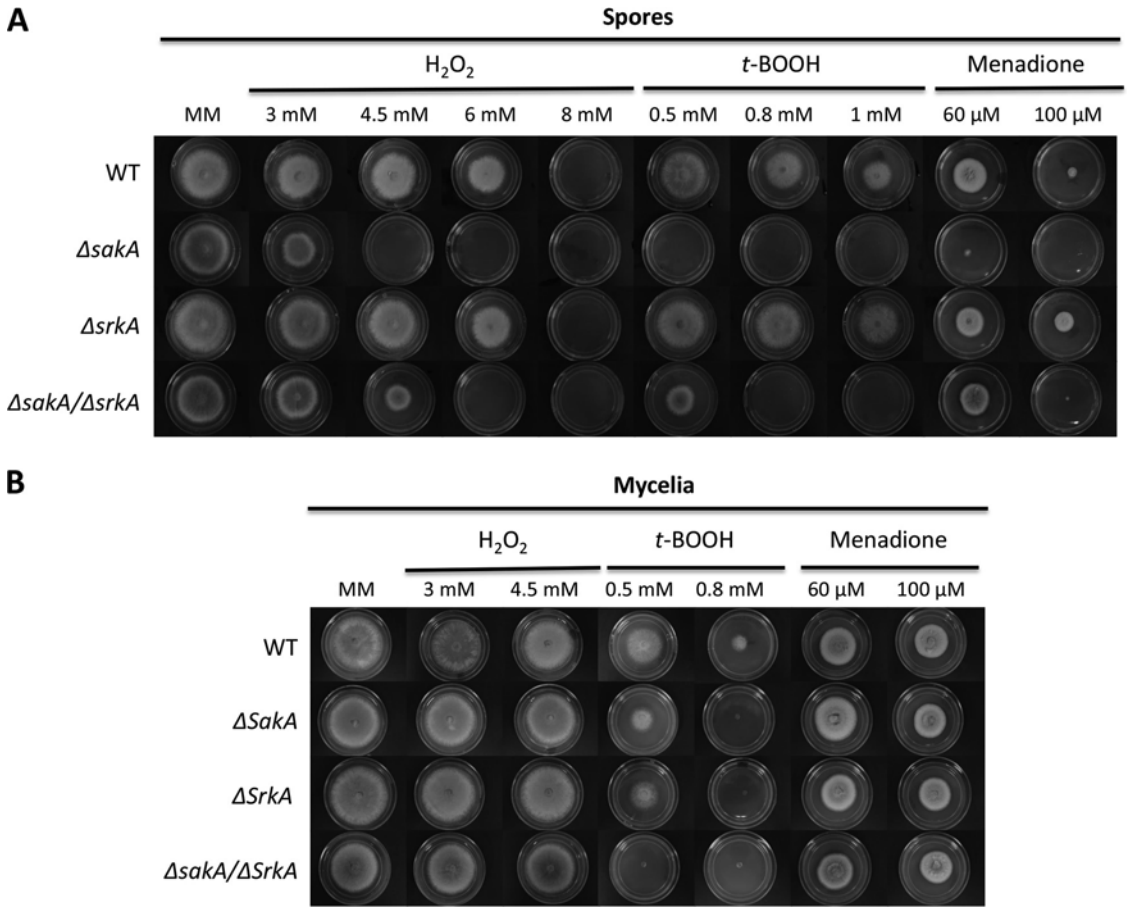

FIG 1 Δ*srkA* mutants are not sensitive to oxidative stress, and the lack of *srkA* partially suppresses the H_2O_2 sensitivity of Δ*sakA* mutant conidia. (A) Conidia (1×10^4) from strains CLK43 (WT), TOL1 (Δ*sakA*), CR2 (Δ*srkA*), and CRJ5 (Δ*sakA* Δ*srkA*) were inoculated on supplemented minimal medium plates containing hydrogen peroxide (H_2O_2), *t*-butyl-hydroperoxide (*t*-BOOH), or menadione at the indicated concentrations and incubated at 37°C for 4 days. (B) Mycelial plugs from strains CLK43, TOL1, CRJ2, and CRJ5 cut from the growing edge of 5-day colonies were transferred to plates containing the indicated compounds and incubated as for panel A. This experiment was repeated at least three times, with the same results.

from nuclei and was found to be homogenously localized throughout the cytosol. Treatment with 30 mM H_2O_2 resulted in a clear accumulation of SrkA::GFP in nuclei and a redistribution of the nonnuclear signal. In the absence of SakA and H_2O_2, SrkA::GFP nonnuclear localization changed to a nonhomogenous pattern, characterized by the presence of tubular and small-vesicle structures. Notably, in this case H_2O_2 treatment did not result in SrkA::GFP nuclear accumulation, and instead, the protein was redistributed into round structures throughout the hyphae. These results indicate that SrkA translocates to the nucleus in response to oxidative stress and that both nuclear and nonnuclear localizations of SrkA are determined by the presence of the SakA protein. Since SakA becomes activated during asexual development, we decided to also detect the localization of SrkA in intact conidia. As shown in Fig. 3B, SrkA::GFP appears in a nonhomogenous vesicular pattern, and part of the fluorescence colocalizes with the H2A::mRFP nuclear signal. In a Δ*sakA* background, SrkA is no longer localized in the nucleus, and the protein appears to be localized mainly at the plasma membrane.

In the absence of SakA, the nonnuclear pattern of SrkA::GFP changed from homogenous to reticular structures that became granular after H_2O_2 treatment (Fig. 3A). A similar change from network and filaments to punctuate units has been reported to occur in mitochondria during ageing in *Podospora anserina* and *S. cerevisiae*, where decreased mitochondrial fission has been linked to extended life span (41). This led us to test if H_2O_2 can induce mitochondrial fission in *A. nidulans* and if SrkA could be partially localized in mitochondria, by using the red fluorescent dye MitoTracker to stain mitochondria in living cells treated with H_2O_2 or left untreated. Results in Fig. 4 show that, indeed, a 30-min treatment of the wild-type strain with H_2O_2 induced a drastic change in mitochondrial morphology, probably caused by a fission process, and a similar phenomenon was observed in strains containing SrkA::GFP, particularly when SakA was not present. As shown in Fig. 4 (bottom [arrowheads]), H_2O_2 induced very similar patterns of fragmentation for both SrkA::GFP and mitochondria, which colocalized in many but not all cases. To learn more about the kinetics of H_2O_2-induced mitochondrial fragmentation, we carried out a time course analysis. As shown in Fig. 5, in the absence of H_2O_2 the initial reticular mitochondrial morphology was preserved during the course of the experiment. In contrast, H_2O_2 induced mitochondrial fragmentation as early as 5 min, which became more evident after 15 min. We did not observe a recovery of the tubular mitochondrial morphology for as long as 2 h, sug-

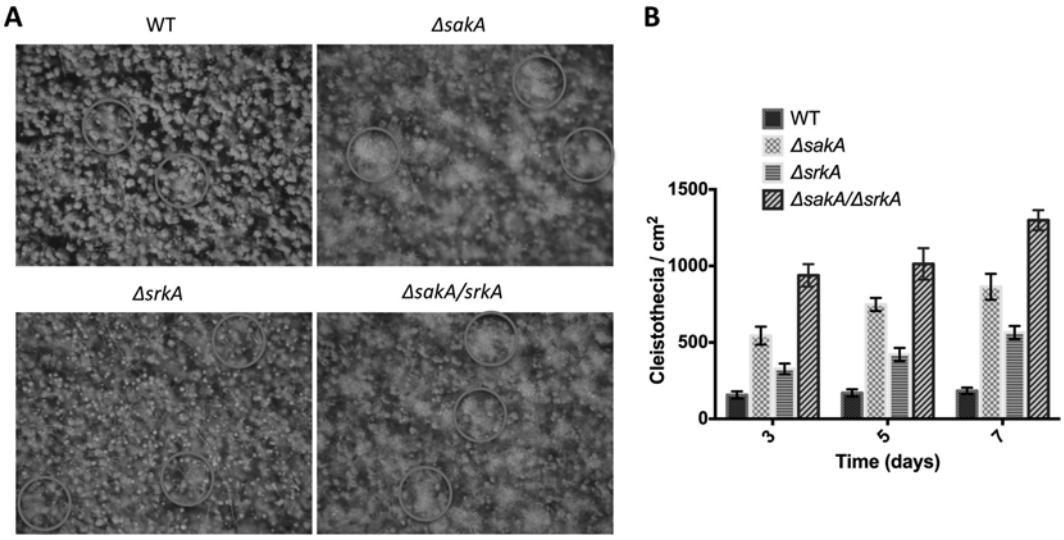

FIG 2 SrkA represses sexual development independently of SakA. (A) Strains CLK43 (WT), TOL1 (Δ*sakA*), CRJ2 (Δ*srkA*), and CRJ5 (Δ*sakA* Δ*srkA*) were induced to undergo sexual development as reported previously (24). Pictures of confluent cultures were taken after 7 days of induction. Circles highlight aggregates of Hülle cells associated with cleistothecium development. (B) The total number of cleistothecia per fixed area was counted under a dissection microscope and used to calculate cleistothecia per square centimeter, as reported elsewhere (24). Data are means from three independent experiments; error bars indicate standard deviations.

gesting that this process is irreversible under these experimental conditions. These results indicate that H_2O_2 induces mitochondrial fragmentation and suggest that H_2O_2 also induces the partial localization of SrkA to mitochondria particularly when SakA is not present. This is consistent with the presence of a highly conserved mitochondrion-targeting signal in SrkA homologs from filamentous fungi (see Fig. S1 in the supplemental material). As fragmented mitochondria are often related to mitophagy, autophagy, and/or apoptosis, further research would be required to determine the possible involvement of SakA and SrkA in these processes.

SrkA and SakA show physical interaction independently of SakA phosphorylation. The above results suggest that without stress, SrkA interacts with SakA outside the nucleus when SakA is not phosphorylated and that SakA activation results in translocation of both proteins to the nucleus. To directly address this possibility, we generated strains in which either *srkA* or *sakA* genes were replaced by alleles that result in tagging of the proteins with the S-tag epitope (39). After confirming the strains and showing that S-tagging did not affect SrkA or SakA functions (see Fig. S6 and S7 in the supplemental material), we carried out protein pulldown experiments (see Materials and Methods) to identify the interaction patterns of both proteins by Western blot and mass spectrometry assays. Protein extracts were prepared from WT, SakA::S-tag, and SrkA::S-tag strains that were untreated or were treated with 10 mM H_2O_2 at different times. S-tag purified proteins were used for Western blot analysis using antibodies that specifically recognize phosphorylated SakA, nonphosphorylated SakA, or the S-tag. Results in Fig. 6 show that pulldown of SrkA::S-tag results in copurification of SakA only in the strain expressing SrkA::S-tag and not in a WT strain. Moreover, results show that this interaction occurs even in the absence of SakA phosphorylation (without H_2O_2). We showed before that nonphosphorylated SakA is excluded from nuclei in the absence of oxidative stress and that H_2O_2 treatment induces SakA phosphorylation and its translocation to the nucleus (25). Our results show that under nonstressing conditions, SrkA interacts physically with nonphosphorylated SakA, while oxidative stress leads to SakA phosphorylation and the localization of both proteins in the nucleus.

Different sets of proteins interact with SakA and/or SrkA in the absence and in the presence of H_2O_2. To confirm the physical interaction between SrkA and SakA and identify other SakA-interacting proteins, we decided to carry out reciprocal pulldown experiments using protein extracts from strains TFL22 and TRJ2, expressing SakA::S-tag and SrkA::S-tag, respectively, together with mass spectrometry analysis. Purified protein extracts were separated in an SDS-acrylamide gel and stained with silver reagent. As shown in Fig. 7A, lanes corresponding to extracts from SakA::S-tag and SrkA::S-tag have enriched bands corresponding to SakA and SrkA molecular masses of 45 and 70 kDa, respectively, while the WT extract shows only faint, unspecific bands. Proteins excised from the SDS gel were processed for mass-spectrometric analysis as reported elsewhere (42). After subtracting common proteins also detected in WT extracts, we used the *Aspergillus* genome database AspGD (47, 48), gene ontology terms, and manual annotation to identify and group the proteins that copurified with SakA and/or SrkA.

The proteins that copurified with SakA or SrkA before and after the H_2O_2 treatment are listed in Table S1 in the supplemental material, Overall, these results indicate that SakA interacts with 57 proteins, of which 21 were detected only after H_2O_2 treatment, 15 were detected only in the absence of H_2O_2, and 21 were common to both sets.

In the case of SrkA, the results suggest that SrkA interacts with 6 proteins without oxidative stress and with 50 proteins in response to H_2O_2 and that 5 of these proteins are common to both sets. Only 1 of the proteins (AcuN) that copurified with SrkA was specific to no H_2O_2 treatment. In contrast, 45 pro-

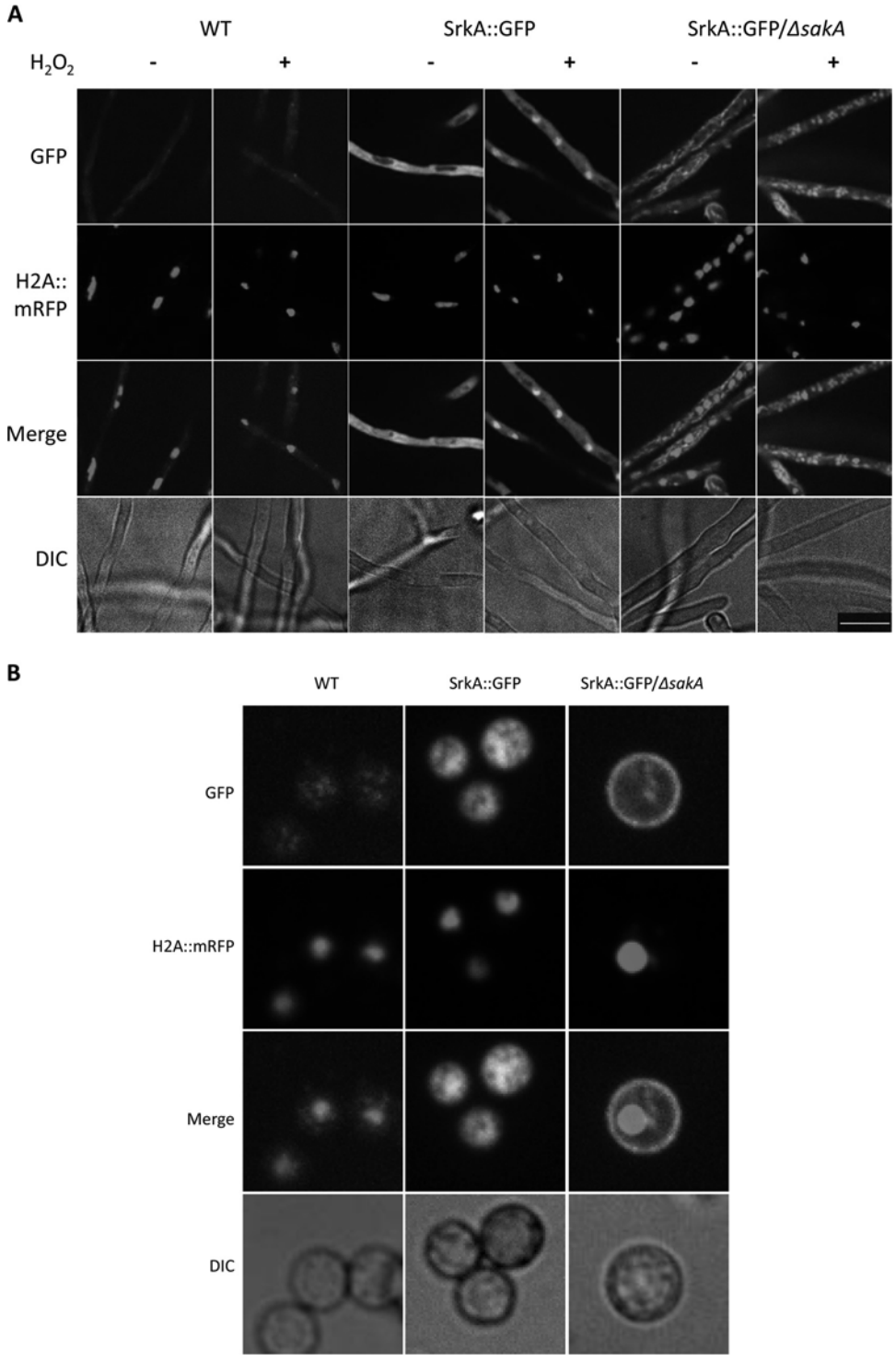

FIG 3 SrkA nuclear localization depends on the presence of SakA. (A) Conidia from strains TRJ7 (WT), TRJ5 (SrkA::GFP), and TRJ6 (SrkA::GFP/Δ*sakA*) were grown for 12 h in minimal medium at 37°C and then exposed to 30 mM H_2O_2 for 30 min and observed *in vivo* using confocal spinning disc microscopy. (B) Intact conidia from strains TRJ7 (WT), TRJ5 (SrkA::GFP), and TRJ6 (SrkA::GFP/Δ*sakA*) were observed using confocal spinning disc microscopy.

teins were detected as interacting with SrkA only upon H_2O_2 treatment (see Table S1 in the supplemental material). Considering SakA and SrkA results together, 14 of the proteins that copurified with SrkA only in the presence of H_2O_2 were also found to copurify with SakA under H_2O_2 conditions, suggesting that they represent specific H_2O_2-induced interactions. Likewise, the proteins recovered from H_2O_2-treated and untreated SakA::S-tag (21 proteins) and SrkA::S-tag (5 proteins) extracts might be considered constitutively associated with the SakA-SrkA protein complex.

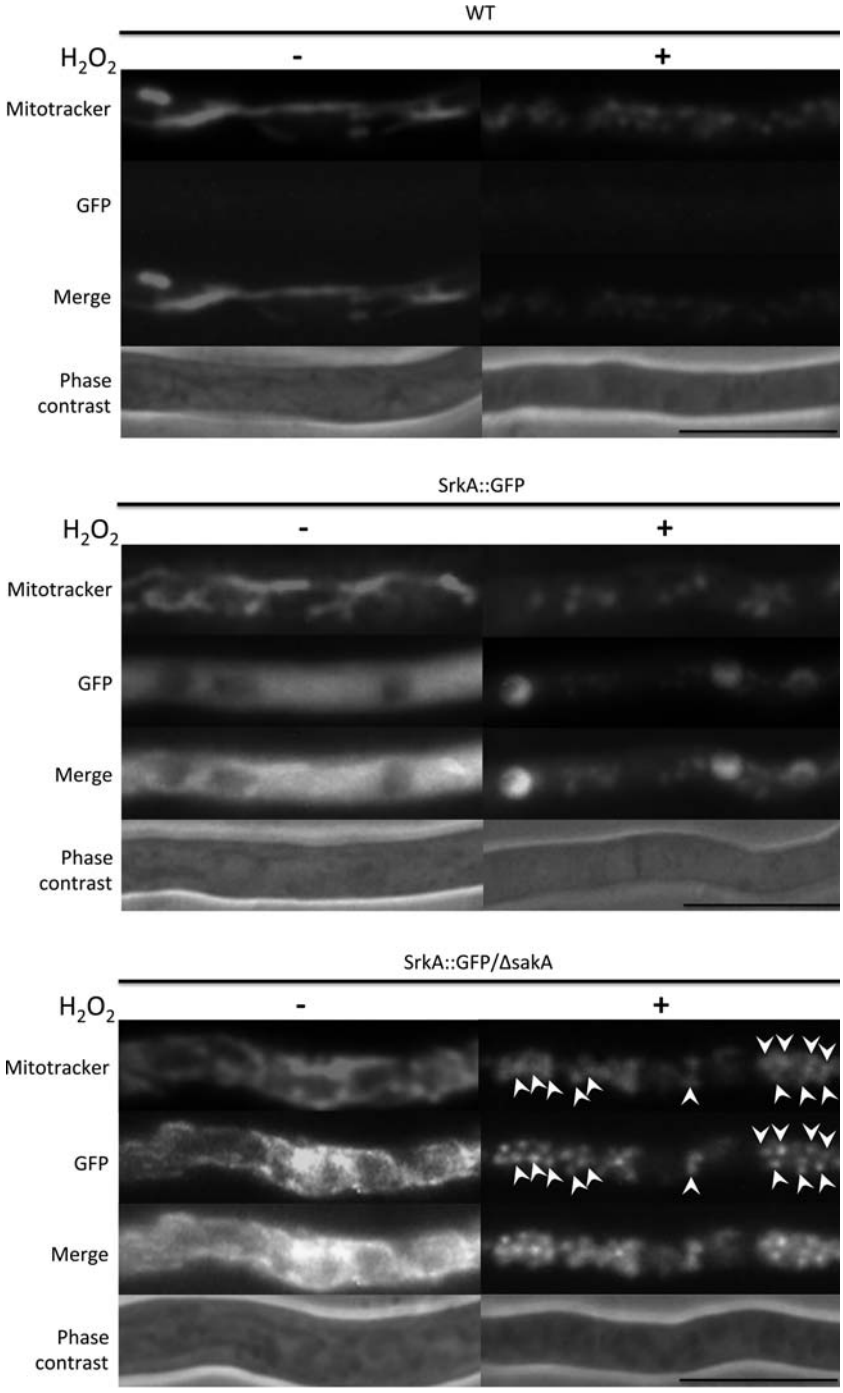

FIG 4 H_2O_2 induces mitochondrial fragmentation and mitochondrial relocalization of SrkA. Strains CLK43 (WT), TRJ1 (SrkA::GFP), and CRJ3 (SrkA::GFP/Δ*sakA*) were incubated with MitoTracker for 5 min, treated with 30 mM H_2O_2 for 30 min or left untreated, and observed *in vivo* using epifluorescence microscopy. Arrowheads highlight some of the regions where Mitotracker and SrkA::GFP signals colocalize. Bar = 10 μm.

SakA interacts with the SrkA kinase, the stress MAPK MpkC, the protein tyrosine phosphatase (PTP) PtpA, and other proteins that can be linked to SakA and SrkA functions. Among the proteins considered constitutively associated with SakA, 17 and 18 peptide sequences corresponding to SrkA (AN4483) were identified under no-stress and oxidative-stress conditions, respectively. Consistent with this, 10 and 12 SakA (AN1017) peptide sequences were identified in non-H_2O_2-treated and H_2O_2-treated SrkA extracts, respectively. These results confirm that SrkA is as a major SakA interactor even in the absence of H_2O_2 and validate our approach to identify SakA and SrkA interacting proteins.

Other proteins that copurified with SakA or SrkA include several potential interactors that can be clearly connected to the func-

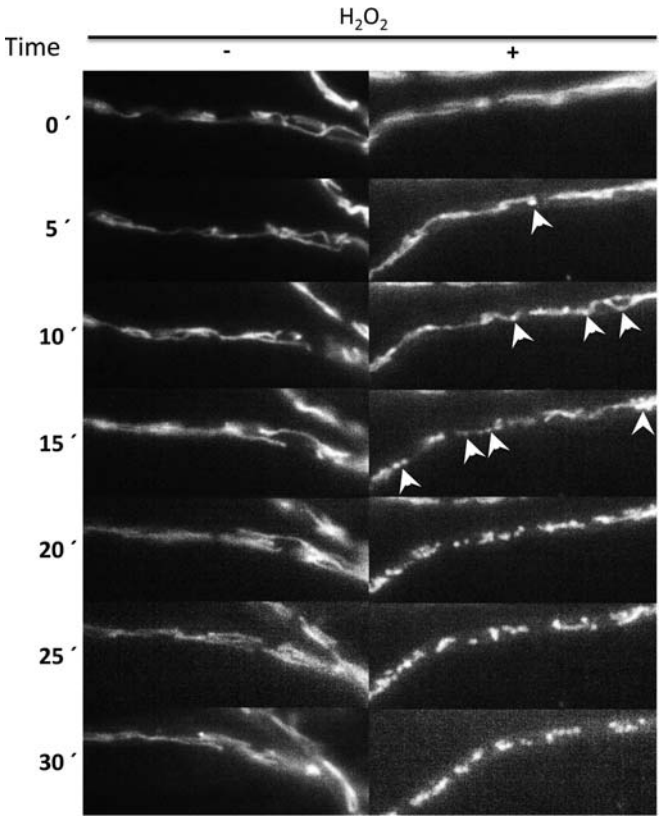

FIG 5 Time course of mitochondrial fragmentation induced by H_2O_2 treatment. Mitochondria from wild-type strain CLK43 were stained with MitoTracker and treated with 30 mM H_2O_2 or left untreated, and single hyphae were photographed every 5 min under epifluorescence microscopy. Arrowheads highlight early fragmented mitochondria.

tions of these kinases. These comprise MpkC (AN4668), a stress MAPK homologous to SakA that, like SakA, is a substrate of the upstream MAPKK PbsB (46), and the PTP PtpA (AN6982), which is homologous to *S. pombe* Pyp2, involved in dephosphorylation of SakA homolog StyI/Spc1 (49). Both MpkC and PtpA were found to be associated with SakA with and without oxidative stress. AN8269, AN6089, and AN2026 are three putative heat shock proteins identified in the SakA and/or SrkA interactomes (see Table S1 in the supplemental material). AN8269, found to be constitutively associated with SakA and SrkA, corresponds to chaperone HSP90, which plays signal transduction functions in many organisms and has been found to interact with Hog1 (50) and be involved in cell cycle progression in *C. albicans* (51).

Among the H_2O_2-specific proteins (Table 3), AN7254, an ortholog of the *S. cerevisiae* Cdc48 ATPase that regulates numerous cellular processes, including protein quality control, DNA repair, and the cell cycle (52), was identified as interaction partner of SakA and SrkA only in the presence of H_2O_2. Consistent with this, AN7254 is induced by conditions that result in SakA activation, such as osmoadaptation (53), farnesol treatment (54), and nutrient starvation (55).

ArtA (AN4501) was found as a SakA-interacting protein and AN5744 as a SrkA interaction partner. ArtA and AN5744 are two of three 14-3-3 signal transduction proteins present in the *A. nidulans* genome, and both are homologs of *S. pombe* Rad24/Rad25. Rad24 is directly related to Srk1 function in *S. pombe* (17), while ArtA is induced by H_2O_2 in *A. fumigatus* and by compounds that induce DNA damage in *A. nidulans* (56).

In response to H_2O_2, SakA and SrkA were also found to be associated with other proteins involved in the response to different types of stress, such as the response to DNA damage, mRNA stability, and protein biosynthesis and mitochondrial function and energy metabolism (Table 3). We think most of these proteins are connected to SakA and SrkA functions (see Discussion).

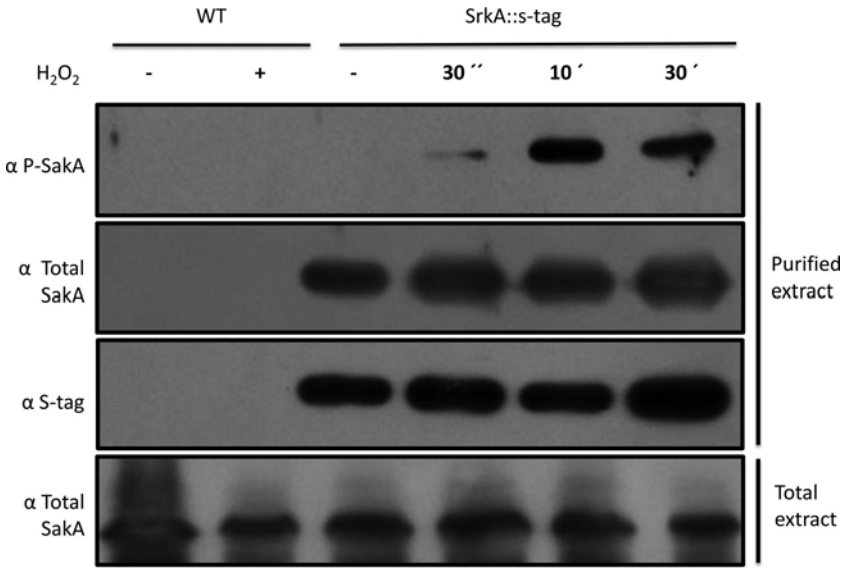

FIG 6 SrkA and SakA interact independently of the SakA phosphorylation state. Mycelia from strains 1155 (WT) and TRJ2 (SrkA::S-tag) were treated with 10 mM H_2O_2 for the indicated times or left untreated, immediately frozen with liquid nitrogen, and processed for S-tag protein purification as described previously (40). Samples (30 μg) were processed for immunoblotting using anti-phospho-P38 (αP-SakA), anti-Hog1 (α Total SakA), and anti-S-tag (α S-tag) antibodies. A blot from the crude extracts using anti-Hog1 (α Total SakA) is included as a protein loading control.

A

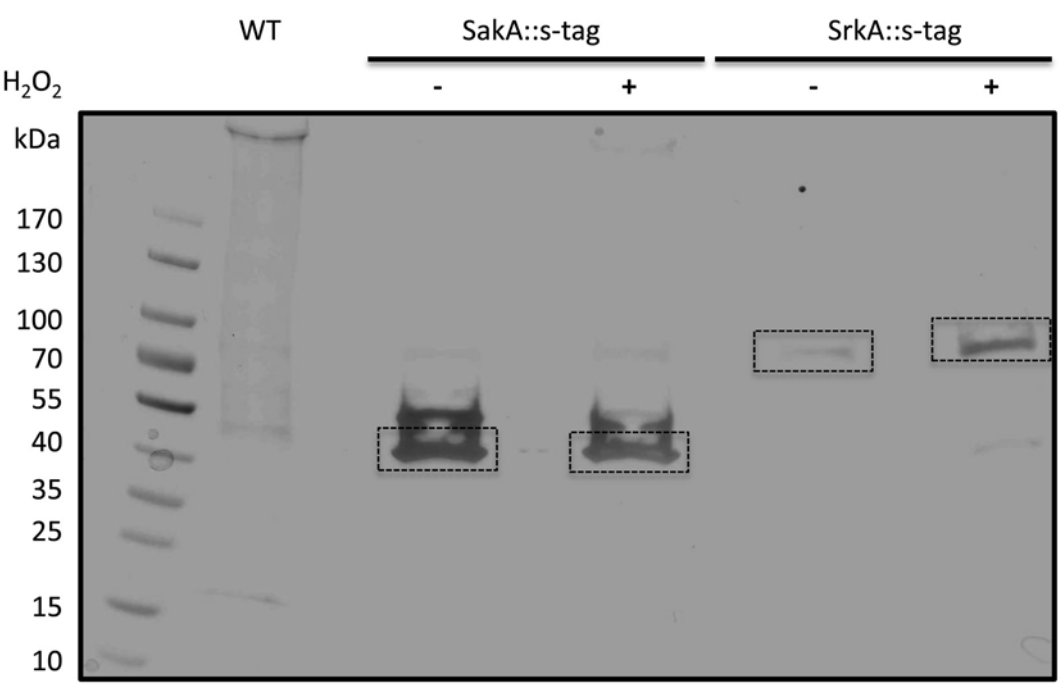

B

H2O2 10mM	SakA::s-tag		SrkA::-s-tag	
	-	+	-	+
Identified peptides	SrkA (AN4483)	SrkA (AN4483)	SakA (AN1017)	SakA (AN1017)
	MGDGAFSNVYR	APFELSLDNASLLEK	AQIFGTTFEITSR	AMLVYNPK
	AIEYLHETSGVVHR	MGDGAFSNVYR	IQDPQMTGYVSTR	ICDFGLAR
	MGDGAFSNVYR	GQYTFLSPWWDDISK	YTDLQPVGMGAFGLVCSAR	AMLVYNPK
	APFELSLDNASLLEK	QPQGQFAPAAGNLDAIDSK	DQLTAQPVAVK	FLALVHPDK
	QPQGQFAPAAGNLDAIDSK	AKDASGEYGEVAIK	IQDPQMTGYVSTR	LISSRPLEK
	AKDASGEYGEVAIK	QTNLGATSHAAQMR	AMLVYNPK	DQLTAQPVAVK
	EAEIEQIIAEEK	QSGEETQAASDAPPLTTPAPEAR	ICDFGLAR	APEIMLTWQK
	GAGGIGVIK	DASGEYGEVAIK	ISAEAALAAPYLAPYHDETDEPVAE	APEIMLTWQK
	QTNLGATSHAAQMR	MGDGAFSNVYR	FDWSFNDADLPVDTWK	DQLTAQPVAVKK
	QSGEETQAASDAPPLTTPAPEAR	AIEYLHETSGVVHR	DLKPSNILINENCDLK	AQIFGTTFEITSR
	DASGEYGEVAIK	VDEGEFIPGK		IQDPQMTGYVSTR
	DLISHLLTVDPDER	LVTPHAEPTTNVSPVHAEQQR		IQDPQMTGYVSTR
	LVTPHAEPTTNVSPVHAEQQR	GAGGIGVIK		DLKPSNILINENCDLK
	DIKPENLLFYPTEYVPSK	STLSDSLVSR		YTDLQPVGMGAFGLVCSAR
	IADFGLSK	DLISHLLTVDPDER		YTDLQPVGMGAFGLVCSAR
	GQYTFLSPWWDDISK	LTYFSEDLSR		ISAEAALAAPYLAPYHDETDEPVAEEK
	EVFDVGYAVHR	QPGDEDKVDEGEFIPGK		
		DIKPENLLFYPTEYVPSK		
		MPHYPGLER		
		EVFDVGYAVHR		
		SPGAINLR		
		IADFGLSK		
		YVLLEK		
		QSNPTAAFQSALNPLDEDYDDEDGIAYQTIDEEGHPPAK		
		AREAEIEQIIAEEK		

FIG 7 SrkA is part of the SakA interactome. (A) SDS-polyacrylamide gel stained with silver reagent, using S-tag purified protein extracts from WT, SakA::S-tag, and SrkA::S-tag protein extracts. Mycelia from strains 1155 (WT), TFL22 (SakA::S-tag), and TRJ2 (SrkA::S-tag) were treated with 10 mM H_2O_2 for 10 min or left untreated, immediately frozen with liquid nitrogen, and processed for S-tag protein purification as described previously (40). (B) Peptides identified by mass spectrometry using samples from lanes excised from the SDS gel shown in panel A.

In summary, we have demonstrated that SakA and SrkA show both functional and physical interactions and that the SakA-SrkA pathway plays differential roles in the antioxidant response and development. We have also shown that H_2O_2 induces mitochondrial fragmentation, consistent with a fission process, and the relocalization of SrkA to nuclei and mitochondria, depending on the presence of SakA. Moreover, we identified potentially new protein targets for SakA and SrkA, suggesting novel functions for these kinases.

DISCUSSION

SrkA inactivation partially suppresses the sensitivity of Δ*sakA* mutant conidia to oxidative stress. Our results show that *A. nidulans* mutants lacking the CAMK SrkA are not sensitive to os-

TABLE 3 Proteins that interact with SakA and/or SrkA in response to H_2O_2

Putative function and protein ID	Protein name and/or description	No. of peptides[a]	
		SakA	SrkA
Cell cycle/signal transduction			
AN7254	Protein with a conserved CDC48, cell division protein N-terminal domain	3	2
AN4501	ArtA, putative 14-3-3 protein	2	
AN5744	Putative 14-3-3-like protein		2
Histone/DNA damage response			
AN0734	H4.1, histone H4.1	3	3
AN3468	H2A.X, histone H2A	2	2
AN3469	H2B, histone H2B; core histone protein		2
Protein biosynthesis/mRNA stability			
AN10416	Putative 60S ribosomal protein		2
AN1964	Ortholog of *S. cerevisiae* RPS6B and RPS6A; *palA*-dependent expression	3	
AN10681	Ortholog(s) has structural constituent of ribosome activity	2	2
AN10740	Has domain(s) with predicted structural constituent of ribosome activity		2
AN4475	Ortholog(s) has role in ribosomal large subunit assembly		2
AN4916	Ortholog(s) has role in ribosome biogenesis		2
AN2275	Ortholog(s) has structural constituent of ribosome activity		2
AN0843	Ortholog(s) has structural constituent of ribosome activity		2
AN4000	FabM protein with similarity to poly(A)-binding proteins		2
AN2932	AN2932, putative eukaryotic initiation factor 4A		2
AN5931	Putative ATP-dependent RNA helicase	4	
Energy metabolism/mitochondrial function			
AN2435	AclA, putative ATP citrate synthase	4	3
AN9403	PdhC, putative pyruvate dehydrogenase (lipoamide)	2	4
AN8979	AlcA, Alcohol dehydrogenase with a role in two-carbon compound metabolism	2	2
AN6717	MdhA, putative mitochondrial malate dehydrogenase	2	
AN4888	PdcA, putative pyruvate decarboxylase		3
AN8275	CitA, mitochondrial citrate synthase		2
AN1534	Putative F_oF_1-ATPase complex subunit		2
AN9340	TreA, α,α-trehalase with a role in trehalose hydrolysis	2	2
Fatty acid metabolism			
AN9408	FasB, fatty acid synthase, beta subunit	2	
Unclassified			
AN4463	Ortholog(s) has structural molecular activity	2	
AN8870	Expression increased in salt-adapted strains	2	2
AN3804	Ortholog(s) has IgE binding activity	2	2
AN4865	Has domain(s) with predicted nucleic acid binding	2	2
AN7725	PyroA protein required for biosynthesis of pyridoxine	2	2
AN0745	Putative nucleolar protein	2	2
AN1551	BtgE putative beta-glucosidase with predicted role in degradation of glucans	2	3

[a] Number of peptides from each protein identified in the sample.

motic, oxidative, or cell wall stress and that SrkA does not mediate the sensitivity to the fungicide fludioxonil. This is in contrast to what occurs in some other fungi, where SrkA orthologs are important in dealing with different types of stress. In *S. cerevisiae* Δ*rck2* mutants are sensitive to oxidative stress (19). In *Cryptococcus neoformans*, Hrk1 has Hog1-dependent and -independent functions and Δ*hrk1* mutants are resistant to fludioxonil and not affected in virulence (57). In *C. albicans*, CaRck2 is required for cell wall stress resistance, although its kinase activity does not seem necessary for this function. In contrast, CaRck2 protein and kinase activity are required for normal virulence in mice (22). In *S. pombe*, there is some controversy as to whether (17) or not (18) Δ*srk1* mutants are sensitive to osmotic stress. Nevertheless, part of our results seem more comparable to what has been found in this yeast, where Srk1 is a substrate of the MAPK StyI and upon different types of stress Srk1 translocates from the cytoplasm to the nucleus, in a StyI-dependent process (18). We found not only that SrkA is not required for stress resistance but also, more importantly, that its elimination results in partial rescue of the oxidative-stress sensitivity of Δ*sakA* strains. Based on this, and the fact that in response to H_2O_2 SakA and SrkA interact with proteins involved in cell cycle control and the DNA damage stress response, we propose that SrkA mediates a decreased survival response in response to oxidative stress (see below).

SrkA represses sexual development independently of SakA. Like the *S. pombe* StyI-Srk1 pair, *A. nidulans* SakA-SrkA equivalent partners are involved in regulation of sexual development. However, the specific roles they play in each fungus are different. StyI elimination results in impaired sexual development and hyperactivation of meiosis only under nitrogen starvation conditions (18). Our results show that SakA as well as SrkA inactivation results in increased sexual differentiation in an additive way, indicating that SakA and SrkA use different pathways to repress sexual development. This, and the fact that SrkA elimination rescues the sensitivity of Δ*sakA* mutants to oxidative stress, indicates that SakA and SrkA interact in a complex, not completely epistatic fashion. Part of this complexity might be related to the fact that among the ascomycetes, only the aspergilli contain a second stress MAPK, called MpkC, which we identified here as a SakA interactor.

H_2O_2 induces a dramatic change in mitochondrial morphology and the relocalization of SrkA during oxidative stress, and asexual development depends on the presence of SakA. We have shown that H_2O_2 induces both a mitochondrial fragmentation consistent with a fission process and the relocalization of SrkA to nuclei and mitochondria. By analogy to what is known to occur in *S. pombe* (17, 58), nuclear SrkA would be involved in stress-induced cell cycle arrest. During *A. nidulans* asexual development, SakA is phosphorylated in conidia and partially localized in the nucleus, where it interacts with the transcription factor AtfA. More importantly, the dephosphorylation of SakA is necessary for spore germination to take place (25). Therefore, the SakA-dependent nuclear localization of SrkA during oxidative stress would be required for the regulation of cell cycle arrest and for the cell cycle arrest and dormancy of conidia. Such activation of the stress MAPK SakA during normal conidiophore and conidium development supports our long-standing view of development as a response to oxidative stress (1, 2).

A mitochondrial localization of yeast SrkA homologs has not been reported before. However, only the SrkA homologs from filamentous fungi contain a conserved mitochondrion-targeting signal (see Fig. S1 in the supplemental material). In addition, recent data show that StyI is partially localized in mitochondria (59), supporting a link between this MAPK pathway and mitochondrial function. The roles of SakA and SrkA in the regulation of mitochondrial function are yet to be determined. However, this hypothesis is supported by the major role that SakA plays in responding to oxidative stress, together with the fact that H_2O_2 induces SakA phosphorylation, mitochondrial fragmentation, SrkA mitochondrial localization, and the interaction of SakA and/or SrkA with mitochondrial proteins (see below). Direct connections between MAPK signaling and mitochondrial dynamics have been reported very recently in mammalian cells, where stress-induced JNK phosphorylation of mitofusin MFN2, involved in mitochondrial fusion, and ERK2 phosphorylation of dynamin-related protein 1 (DRP1), required for mitochondrial fission, both result in mitochondrial fragmentation (60, 61).

SakA and SrkA interact with each other and with proteins involved in cell cycle regulation and DNA damage response. Our proteomic experiments not only confirmed SakA-SrkA interaction but also identified 33 proteins that potentially interact with SakA and/or SrkA upon oxidative-stress treatment. It is clear that these interactions need to be confirmed using other methods, as some could represent false positives. However, we discuss them in some detail because some of these proteins can be directly linked to SakA and SrkA functions, while others represent potential new targets involved in the response to different types of stress, such as the response to DNA damage, carbon or nitrogen limitation and regulation of the cell cycle. Functions that are all consistent with SakA roles in osmotic, oxidative, and nutrient starvation stress responses (24, 25).

The proteins that might be directly related to SakA and/or SrkA functions include the stress MAPK MpkC (AN4668) and the PTP PtpA (AN6982). In *A. fumigatus*, MpkC is required for the utilization of sorbitol and mannitol as sole carbon sources (62), and although *A. nidulans* Δ*mpkC* mutants do not show any clear phenotype (63), MpkC is the substrate of the SakA-upstream MAPKK PbsB (64). MpkC and SakA belong to the same family of stress MAPKs, and SrkA could also be a MpkC substrate. As MpkC was found to be continuously associated with SakA (stress and no stress), it is likely that in response to H_2O_2, MpkC could be translocated to the nucleus along with SakA. SakA and/or MpkC could be substrates of the PTP PtpA (AN6982), and although mutants lacking PtpA do not show any clear phenotype (65), they have not been characterized in detail yet.

Notably, AN5744 (SrkA interacting) and AN4501 (ArtA; SakA interacting) correspond to 14-3-3 proteins homologous to *S. pombe* Rad24 and Rad25. In this yeast, the phosphorylation of Cdc25 by Srk1 causes Cdc25 binding to Rad24 (17), and in mammalian cells, protein phosphorylation by the functionally homologous kinase MK2 promotes interaction with different 14-3-3 proteins, some connected to the DNA damage response (66). In *A. nidulans*, the Cdc25 ortholog NimT also controls DNA damage checkpoint, regulating NimX (Cdc2 ortholog) activity (67). AN7254, another potential SakA interactor orthologous to the *S. pombe* cell cycle-regulatory protein Cdc48, could also be related to SakA and SrkA functions in cell cycle control. Upon H_2O_2 treatment, SakA and SrkA also interact with histones H2A.X and H4.1, and SrkA interacts with histone H2B (Table 3). Phosphorylation of H2A.X is recognized as a universal epigenetic signal for DNA double-strand-break repair (68), and H4.1 is also associated with histone deposition and DNA damage repair. We have found that H_2O_2 can induce mitochondrion fragmentation, which in turn could induce an increased production of ROS. Either directly or indirectly, H_2O_2 can induce DNA damage. The oxidative-stress-induced interaction of SakA and SrkA with these histones suggests that these kinases function in chromatin remodeling and DNA repair during oxidative stress, which in turn might be related to SakA and SrkA functions in sexual development and meiosis.

SakA and SrkA interaction with proteins involved in mRNA stability and protein synthesis. Different SrkA homologs play central roles in regulation of mRNA stability and translation. In *S. cerevisiae* Rck2 attenuates global protein synthesis under stress conditions (20, 69). In mammalian cells MK2/3 regulates cytokine mRNA stability and translation (70), and the MAPK-activated protein kinase RSK2 orchestrates stress responses with cell survival and proliferation through the formation of stress granules. Silencing RSK2 reduces stress granule formation by blocking the recruitment of TIA-1 (an RNA-binding protein acting as a translation factor) to stress granules (71). In this context, it is interesting that SakA and/or SrkA interacts with proteins potentially involved in similar processes. Among these, AN5931 corresponds to a putative ATP-dependent RNA helicase, and FabM is a poly(A)-binding protein whose overexpression induces conidiation in *A.*

nidulans (72). AN1068, AN2275, and AN0843 are components of the ribosome, while AN2932 is a putative translation initiation factor. We did not detect interaction of SakA with the transcription factor AtfA, known to interact with SakA (25), perhaps because of weak interactions. However, AN10103, a putative transcription factor of the high-mobility group (HMG) family was identified as constitutively associated with SakA and SrkA. AN10103 is the homolog of *S. cerevisiae* Hmo1, a protein involved in ribosomal protein gene transcription, chromatin organization, and oxygen sensing (73, 74).

SakA- and/or SrkA-interacting proteins involved in mitochondrial function and energy metabolism. In human mesenchyme stem cells, the SakA-homologous MAPK p38 mediates increased mitochondrial activity in an MK2-dependent manner, higher ROS levels, a persistent DNA damage response, DNA double-strand breaks (DSBs), and activation of the ATM pathway. This feedback loop seems necessary to stop the cell cycle and drive cells into senescence (75). Mitochondrial ROS are produced by partial O_2 reduction in the respiratory chain or by damage and loss of membrane potential (76, 77). In the last case, the cell uses a retrograde signaling (RTG) from mitochondria to the nucleus to adjust metabolic and biosynthetic pathways and compensate for the loss of mitochondrial quality (78, 79). Hog1 activates the RTG pathway in yeast at the transcriptional level (80), but a direct interaction or regulation of mitochondrial proteins by this MAPK has not been reported. In this regard, it is interesting that H_2O_2 induces SakA phosphorylation, mitochondrial fragmentation, SrkA mitochondrial localization, and, as discussed here, the interaction of SakA and/or SrkA with proteins involved in mitochondrial function or carbon, nitrogen, or fatty acid metabolism.

In response to H_2O_2, SakA interacts with the mitochondrial proteins citrate synthase (AN2435) and MdhA (AN6717), a putative malate dehydrogenase downregulated upon shift from glucose to ethanol (81). These proteins are predicted to play a role in the trichloroacetic acid (TCA) cycle, being implicated in energy metabolism. Furthermore, SakA interacts constitutively with the aldehyde dehydrogenase AldA (AN0554) and during oxidative stress with the alcohol dehydrogenase AlcA, two enzymes required for ethanol utilization. As the *alcA* and *aldA* genes are normally subject to glucose repression, the presence of these proteins under our experimental conditions is somewhat unexpected. In addition, the fatty acid synthase alpha (FasA) subunit was associated with SakA with and without stress, while the beta (FasB) subunit was associated with SakA and SrkA upon H_2O_2 treatment. Fatty acid synthases are involved in the cytosolic NADPH-consuming synthesis of fatty acids.

SakA also interacts with two proteins involved in nitrogen assimilation, the nitrite reductase NiiA (AN1007) and the glutamate dehydrogenase GdhA (AN4376). GdhA is a critical enzyme linking fundamental metabolic pathways such as amino acid metabolism, TCA cycle, and glutathione biosynthesis. *S. cerevisiae* mutants lacking Gdh3 show accelerated chronological ageing and are hypersensitive to thermal and oxidative stress (82). In *S. pombe*, StyI is activated after nitrogen starvation and promotes meiosis through transcription factor Atf1 (83), but again, a direct interaction or regulation of the enzymes involved in nitrogen metabolism has not been explored.

It is interesting that the abundance of 15 proteins that interact with SakA or SrkA after H_2O_2 exposure is altered by farnesol or menadione treatment (see Table S2 in the supplemental material), as these compounds induce the generation of ROS (84, 85) and provoke apoptosis and cell cycle arrest in yeasts and filamentous fungi (84, 86, 87). In fact, SakA mediates the induction of the *dplA* gene by farnesol, which encodes a putative dehydrin involved in conidium resistance to H_2O_2 (54).

Together, our results support a model in which part of the SrkA pool interacts with nonphosphorylated SakA in the cytosol preventing its accumulation in mitochondria, perhaps by masking its mitochondrial targeting signal. Under oxidative-stress conditions, phosphorylated SakA would phosphorylate bound SrkA, and the interacting proteins would translocate to the nucleus, while a nonnuclear (not bound to SakA) SrkA fraction would interact with stress proteins in the cytoplasm, accumulate in fissioned mitochondria, and interact with proteins involved in mitochondrial function. In the absence of SakA, a larger portion of SrkA accumulates in mitochondria with or without oxidative stress. According to the StyI-Srk1 model (17, 58), SakA and SrkA will dissociate inside the nucleus; SakA will then interact with transcription factor AtfA and other proteins. SrkA will regulate cell cycle arrest through phosphorylation of Cdc25, allowing this protein to interact with the 14-3-3 protein ArtA or AN5744 in order to be excluded from the nucleus. Phosphorylated SrkA inside the nucleus would be prone to degradation.

According to this model, SakA and SrkA are part of an oxidative and general stress signal transduction pathway involved in regulation of the cell cycle, the DNA damage response, stability of mRNA and protein synthesis, and the regulation of energy metabolism and mitochondrial function. Our results provide new insights into the mechanisms of MAPK stress signaling and its connections to fungal development, opening new lines of research in this field.

ACKNOWLEDGMENTS

This work was funded by grants CB-2010-01-153256 from CONACYT, IN207913 from PAPIIT-UNAM, DFG-CONACYT Germany-México Collaboration Grant 75306 from CONACYT, and the Deutsche Forschungsgemeinschaft (DFG; Mexican-German research unit 1334). R. Jaimes-Arroyo is a Ph.D. student in the program Posgrado en Ciencias Biológicas from UNAM and recipient of a fellowship (229044) from CONACYT.

We are deeply grateful to Olivia Sánchez (IFC-UNAM) for her technical support, to Özlem S. Bayram for providing nuclear marker plasmids pOB340 and pON307, and to Luis Cárdenas (IBT-UNAM) for his generous support with *in vivo* imaging. We also thank the Molecular Biology and Microscopy Units (IFC-UNAM) and Juan Barbosa and Ivette Rosas from the IFC Computer Facility.

REFERENCES

1. **Aguirre J, Rios-Momberg M, Hewitt D, Hansberg W.** 2005. Reactive oxygen species and development in microbial eukaryotes. Trends Microbiol **13:**111–118. http://dx.doi.org/10.1016/j.tim.2005.01.007.
2. **Hansberg W, Aguirre J.** 1990. Hyperoxidant states cause microbial cell differentiation by cell isolation from dioxygen. J Theor Biol **142:**201–221. http://dx.doi.org/10.1016/S0022-5193(05)80222-X.
3. **Lara-Ortiz T, Riveros-Rosas H, Aguirre J.** 2003. Reactive oxygen species generated by microbial NADPH oxidase NoxA regulate sexual development in Aspergillus nidulans. Mol Microbiol **50:**1241–1255. http://dx.doi.org/10.1046/j.1365-2958.2003.03800.x.
4. **Cano-Dominguez N, Alvarez-Delfin K, Hansberg W, Aguirre J.** 2008. NADPH oxidases NOX-1 and NOX-2 require the regulatory subunit NOR-1 to control cell differentiation and growth in Neurospora crassa. Eukaryot Cell **7:**1352–1361. http://dx.doi.org/10.1128/EC.00137-08.
5. **Dirschnabel DE, Nowrousian M, Cano-Dominguez N, Aguirre J, Teichert I, Kuck U.** 2014. New insights into the roles of NADPH oxidases in

sexual development and ascospore germination in Sordaria macrospora. Genetics **196:**729–744. http://dx.doi.org/10.1534/genetics.113.159368.

6. **Hernandez-Onate MA, Esquivel-Naranjo EU, Mendoza-Mendoza A, Stewart A, Herrera-Estrella AH.** 2012. An injury-response mechanism conserved across kingdoms determines entry of the fungus Trichoderma atroviride into development. Proc Natl Acad Sci U S A **109:**14918–14923. http://dx.doi.org/10.1073/pnas.1209396109.
7. **Malagnac F, Lalucque H, Lepere G, Silar P.** 2004. Two NADPH oxidase isoforms are required for sexual reproduction and ascospore germination in the filamentous fungus Podospora anserina. Fungal Genet Biol **41:**982–997. http://dx.doi.org/10.1016/j.fgb.2004.07.008.
8. **Ryder LS, Dagdas YF, Mentlak TA, Kershaw MJ, Thornton CR, Schuster M, Chen J, Wang Z, Talbot NJ.** 2013. NADPH oxidases regulate septin-mediated cytoskeletal remodeling during plant infection by the rice blast fungus. Proc Natl Acad Sci U S A **110:**3179–3184. http://dx.doi.org/10.1073/pnas.1217470110.
9. **Siegmund U, Heller J, van Kan JA, Tudzynski P.** 2013. The NADPH oxidase complexes in Botrytis cinerea: evidence for a close association with the ER and the tetraspanin Pls1. PLoS One **8:**e55879. http://dx.doi.org/10.1371/journal.pone.0055879.
10. **Takemoto D, Tanaka A, Scott B.** 2006. A p67Phox-like regulator is recruited to control hyphal branching in a fungal-grass mutualistic symbiosis. Plant Cell **18:**2807–2821. http://dx.doi.org/10.1105/tpc.106.046169.
11. **Aguirre J, Lambeth JD.** 2010. Nox enzymes from fungus to fly to fish and what they tell us about Nox function in mammals. Free Radic Biol Med **49:**1342–1353. http://dx.doi.org/10.1016/j.freeradbiomed.2010.07.027.
12. **Nishiyama R, Watanabe Y, Leyva-Gonzalez MA, Ha CV, Fujita Y, Tanaka M, Seki M, Yamaguchi-Shinozaki K, Shinozaki K, Herrera-Estrella L, Tran LS.** 2013. Arabidopsis AHP2, AHP3, and AHP5 histidine phosphotransfer proteins function as redundant negative regulators of drought stress response. Proc Natl Acad Sci U S A **110:**4840–4845. http://dx.doi.org/10.1073/pnas.1302265110.
13. **Aguirre J, Hansberg W, Navarro R.** 2006. Fungal responses to reactive oxygen species. Med Mycol **44:**S101–S107. http://dx.doi.org/10.1080/13693780600900080.
14. **Buck V, Quinn J, Soto Pino T, Martin H, Saldanha J, Makino K, Morgan BA, Millar JB.** 2001. Peroxide sensors for the fission yeast stress-activated mitogen-activated protein kinase pathway. Mol Biol Cell **12:**407–419. http://dx.doi.org/10.1091/mbc.12.2.407.
15. **Nguyen AN, Lee A, Place W, Shiozaki K.** 2000. Multistep phosphorelay proteins transmit oxidative stress signals to the fission yeast stress-activated protein kinase. Mol Biol Cell **11:**1169–1181. http://dx.doi.org/10.1091/mbc.11.4.1169.
16. **Sukegawa Y, Yamashita A, Yamamoto M.** 2011. The fission yeast stress-responsive MAPK pathway promotes meiosis via the phosphorylation of Pol II CTD in response to environmental and feedback cues. PLoS Genet **7:**e1002387. http://dx.doi.org/10.1371/journal.pgen.1002387.
17. **Lopez-Aviles S, Lambea E, Moldon A, Grande M, Fajardo A, Rodriguez-Gabriel MA, Hidalgo E, Aligue R.** 2008. Activation of Srk1 by the mitogen-activated protein kinase StyI/Spc1 precedes its dissociation from the kinase and signals its degradation. Mol Biol Cell **19:**1670–1679. http://dx.doi.org/10.1091/mbc.E07-07-0639.
18. **Smith DA, Toone WM, Chen D, Bahler J, Jones N, Morgan BA, Quinn J.** 2002. The Srk1 protein kinase is a target for the StyI stress-activated MAPK in fission yeast. J Biol Chem **277:**33411–33421. http://dx.doi.org/10.1074/jbc.M204593200.
19. **Bilsland E, Molin C, Swaminathan S, Ramne A, Sunnerhagen P.** 2004. Rck1 and Rck2 MAPKAP kinases and the HOG pathway are required for oxidative stress resistance. Mol Microbiol **53:**1743–1756. http://dx.doi.org/10.1111/j.1365-2958.2004.04238.x.
20. **Teige M, Scheikl E, Reiser V, Ruis H, Ammerer G.** 2001. Rck2, a member of the calmodulin-protein kinase family, links protein synthesis to high osmolarity MAP kinase signaling in budding yeast. Proc Natl Acad Sci U S A **98:**5625–5630. http://dx.doi.org/10.1073/pnas.091610798.
21. **Swaminathan S, Sunnerhagen P.** 2005. Degradation of Saccharomyces cervisiae Rck2 upon exposure of cells to high levels of zinc is dependent on Pep4. Mol Genet Genomics **273:**433–439. http://dx.doi.org/10.1007/s00438-005-1151-8.
22. **Li X, Du W, Zhao J, Zhang L, Zhu Z, Jiang L.** 2010. The MAP kinase-activated protein kinase Rck2p regulates cellular responses to cell wall stresses, filamentation and virulence in the human fungal pathogen Candida albicans. FEMS Yeast Res **10:**441–451. http://dx.doi.org/10.1111/j.1567-1364.2010.00626.x.
23. **Vargas-Perez I, Sanchez O, Kawasaki L, Georgellis D, Aguirre J.** 2007. Response regulators SrrA and SskA are central components of a phospho-relay system involved in stress signal transduction and asexual sporulation in Aspergillus nidulans. Eukaryot Cell **6:**1570–1583. http://dx.doi.org/10.1128/EC.00085-07.
24. **Kawasaki L, Sanchez O, Shiozaki K, Aguirre J.** 2002. SakA MAP kinase is involved in stress signal transduction, sexual development and spore viability in Aspergillus nidulans. Mol Microbiol **45:**1153–1163. http://dx.doi.org/10.1046/j.1365-2958.2002.03087.x.
25. **Lara-Rojas F, Sanchez O, Kawasaki L, Aguirre J.** 2011. Aspergillus nidulans transcription factor AtfA interacts with the MAPK SakA to regulate general stress responses, development and spore functions. Mol Microbiol **80:**436–454. http://dx.doi.org/10.1111/j.1365-2958.2011.07581.x.
26. **Han KH, Prade RA.** 2002. Osmotic stress-coupled maintenance of polar growth in Aspergillus nidulans. Mol Microbiol **43:**1065–1078. http://dx.doi.org/10.1046/j.1365-2958.2002.02774.x.
27. **Hagiwara D, Asano Y, Marui J, Yoshimi A, Mizuno T, Abe K.** 2009. Transcriptional profiling for Aspergillusnidulans HogA MAPK signaling pathway in response to fludioxonil and osmotic stress. Fungal Genet Biol **46:**868–878. http://dx.doi.org/10.1016/j.fgb.2009.07.003.
28. **Eaton CJ, Jourdain I, Foster SJ, Hyams JS, Scott B.** 2008. Functional analysis of a fungal endophyte stress-activated MAP kinase. Curr Genet **53:**163–174. http://dx.doi.org/10.1007/s00294-007-0174-6.
29. **Heller J, Ruhnke N, Espino JJ, Massaroli M, Collado IG, Tudzynski P.** 2012. The mitogen-activated protein kinase BcSak1 of Botrytis cinerea is required for pathogenic development and has broad regulatory functions beyond stress response. Mol Plant Microbe Interact **25:**802–816. http://dx.doi.org/10.1094/MPMI-11-11-0299.
30. **Lamb TM, Finch KE, Bell-Pedersen D.** 2012. The Neurospora crassa OS MAPK pathway-activated transcription factor ASL-1 contributes to circadian rhythms in pathway responsive clock-controlled genes. Fungal Genet Biol **49:**180–188. http://dx.doi.org/10.1016/j.fgb.2011.12.006.
31. **Nimmanee P, Woo PC, Kummasook A, Vanittanakom N.** 2015. Characterization of sakA gene from pathogenic dimorphic fungus Penicillium marneffei. Int J Med Microbiol **305:**65–74. http://dx.doi.org/10.1016/j.ijmm.2014.11.003.
32. **Van Nguyen T, Kroger C, Bonnighausen J, Schafer W, Bormann J.** 2013. The ATF/CREB transcription factor Atf1 is essential for full virulence, deoxynivalenol production, and stress tolerance in the cereal pathogen Fusarium graminearum. Mol Plant Microbe Interact **26:**1378–1394. http://dx.doi.org/10.1094/MPMI-04-13-0125-R.
33. **Hill TW, Kafer E.** 2001. Improved protocols for Aspergillus minimal medium: trace element and minimal medium salt stock solution. Fungal Genet Newsl **48:**20–21.
34. **Han KH, Park JS, Chae KS, Han DM.** 2010. Simple identification of *veA1* mutation in *Aspergillus nidulans*. J Microbiol **48:**885–887. http://dx.doi.org/10.1007/s12275-010-0506-y.
35. **Yu JH, Hamari Z, Han KH, Seo JA, Reyes-Dominguez Y, Scazzocchio C.** 2004. Double-joint PCR: a PCR-based molecular tool for gene manipulations in filamentous fungi. Fungal Genet Biol **41:**973–981. http://dx.doi.org/10.1016/j.fgb.2004.08.001.
36. **Nayak T, Szewczyk E, Oakley CE, Osmani A, Ukil L, Murray SL, Hynes MJ, Osmani SA, Oakley BR.** 2006. A versatile and efficient gene-targeting system for Aspergillus nidulans. Genetics **172:**1557–1566. http://dx.doi.org/10.1534/genetics.105.052563.
37. **Punt PJ, van den Hondel CA.** 1992. Transformation of filamentous fungi based on hygromycin B and phleomycin resistance markers. Methods Enzymol **216:**447–457. http://dx.doi.org/10.1016/0076-6879(92)16041-H.
38. **Yang L, Ukil L, Osmani A, Nahm F, Davies J, De Souza CP, Dou X, Perez-Balaguer A, Osmani SA.** 2004. Rapid production of gene replacement constructs and generation of a green fluorescent protein-tagged centromeric marker in Aspergillus nidulans. Eukaryot Cell **3:**1359–1362. http://dx.doi.org/10.1128/EC.3.5.1359-1362.2004.
39. **Liu HL, Osmani AH, Ukil L, Son S, Markossian S, Shen KF, Govindaraghavan M, Varadaraj A, Hashmi SB, De Souza CP, Osmani SA.** 2010. Single-step affinity purification for fungal proteomics. Eukaryot Cell **9:**831–833. http://dx.doi.org/10.1128/EC.00032-10.
40. **Bayram O, Bayram OS, Ahmed YL, Maruyama J, Valerius O, Rizzoli SO, Ficner R, Irniger S, Braus GH.** 2012. The Aspergillus nidulans MAPK module AnSte11-Ste50-Ste7-Fus3 controls development and secondary metabolism. PLoS Genet **8:**e1002816. http://dx.doi.org/10.1371/journal.pgen.1002816.
41. **Scheckhuber CQ, Erjavec N, Tinazli A, Hamann A, Nystrom T,**

Osiewacz HD. 2007. Reducing mitochondrial fission results in increased life span and fitness of two fungal ageing models. Nat Cell Biol **9:**99–105. http://dx.doi.org/10.1038/ncb1524.
42. **Bayram O, Krappmann S, Ni M, Bok JW, Helmstaedt K, Valerius O, Braus-Stromeyer S, Kwon NJ, Keller NP, Yu JH, Braus GH.** 2008. VelB/VeA/LaeA complex coordinates light signal with fungal development and secondary metabolism. Science **320:**1504–1506. http://dx.doi.org/10.1126/science.1155888.
43. **Asp E, Sunnerhagen P.** 2003. Mkp1 and Mkp2, two MAPKAP-kinase homologues in Schizosaccharomyces pombe, interact with the MAP kinase StyI. Mol Genet Genomics **268:**585–597. http://dx.doi.org/10.1007/s00438-002-0786-y.
44. **De Souza CP, Hashmi SB, Osmani AH, Andrews P, Ringelberg CS, Dunlap JC, Osmani SA.** 2013. Functional analysis of the Aspergillus nidulans kinome. PLoS One **8:**e58008. http://dx.doi.org/10.1371/journal.pone.0058008.
45. **Kim H, Han K, Kim K, Han D, Jahng K, Chae K.** 2002. The *veA* gene activates sexual development in *Aspergillus nidulans*. Fungal Genet Biol **37:**72–80. http://dx.doi.org/10.1016/S1087-1845(02)00029-4.
46. **Kaefer E.** 1965. Origins of translocations in *Aspergillus nidulans*. Genetics **52:**217–232.
47. **Cerqueira GC, Arnaud MB, Inglis DO, Skrzypek MS, Binkley G, Simison M, Miyasato SR, Binkley J, Orvis J, Shah P, Wymore F, Sherlock G, Wortman JR.** 2014. The Aspergillus Genome Database: multispecies curation and incorporation of RNA-Seq data to improve structural gene annotations. Nucleic Acids Res **42:**D705–D710. http://dx.doi.org/10.1093/nar/gkt1029.
48. **Galagan JE, Calvo SE, Borkovich KA, Selker EU, Read ND, Jaffe D, FitzHugh W, Ma LJ, Smirnov S, Purcell S, Rehman B, Elkins T, Engels R, Wang S, Nielsen CB, Butler J, Endrizzi M, Qui D, Ianakiev P, Bell-Pedersen D, Nelson MA, Werner-Washburne M, Selitrennikoff CP, Kinsey JA, Braun EL, Zelter A, Schulte U, Kothe GO, Jedd G, Mewes W, Staben C, Marcotte E, Greenberg D, Roy A, Foley K, Naylor J, Stange-Thomann N, Barrett R, Gnerre S, Kamal M, Kamvysselis M, Mauceli E, Bielke C, Rudd S, Frishman D, Krystofova S, Rasmussen C, Metzenberg RL, Perkins DD, Kroken S, et al.** 2003. The genome sequence of the filamentous fungus Neurospora crassa. Nature **422:**859–868. http://dx.doi.org/10.1038/nature01554.
49. **Degols G, Shiozaki K, Russell P.** 1996. Activation and regulation of the Spc1 stress-activated protein kinase in Schizosaccharomyces pombe. Mol Cell Biol **16:**2870–2877.
50. **Hawle P, Horst D, Bebelman JP, Yang XX, Siderius M, van der Vies SM.** 2007. Cdc37p is required for stress-induced high-osmolarity glycerol and protein kinase C mitogen-activated protein kinase pathway functionality by interaction with Hog1p and Slt2p (Mpk1p). Eukaryot Cell **6:**521–532. http://dx.doi.org/10.1128/EC.00343-06.
51. **Senn H, Shapiro RS, Cowen LE.** 2012. Cdc28 provides a molecular link between Hsp90, morphogenesis, and cell cycle progression in Candida albicans. Mol Biol Cell **23:**268–283. http://dx.doi.org/10.1091/mbc.E11-08-0729.
52. **Bohm S, Buchberger A.** 2013. The budding yeast Cdc48(Shp1) complex promotes cell cycle progression by positive regulation of protein phosphatase 1 (Glc7). PLoS One **8:**e56486. http://dx.doi.org/10.1371/journal.pone.0056486.
53. **Kim Y, Nandakumar MP, Marten MR.** 2007. Proteome map of Aspergillus nidulans during osmoadaptation. Fungal Genet Biol **44:**886–895. http://dx.doi.org/10.1016/j.fgb.2006.12.001.
54. **Wartenberg D, Vodisch M, Kniemeyer O, Albrecht-Eckardt D, Scherlach K, Winkler R, Weide M, Brakhage AA.** 2012. Proteome analysis of the farnesol-induced stress response in Aspergillus nidulans–The role of a putative dehydrin. J Proteomics **75:**4038–4049. http://dx.doi.org/10.1016/j.jprot.2012.05.023.
55. **Kim Y, Islam N, Moss BJ, Nandakumar MP, Marten MR.** 2011. Autophagy induced by rapamycin and carbon-starvation have distinct proteome profiles in Aspergillus nidulans. Biotechnol Bioeng **108:**2705–2715. http://dx.doi.org/10.1002/bit.23223.
56. **Malavazi I, Savoldi M, Di Mauro SM, Menck CF, Harris SD, Goldman MH, Goldman GH.** 2006. Transcriptome analysis of Aspergillus nidulans exposed to camptothecin-induced DNA damage. Eukaryot Cell **5:**1688–1704. http://dx.doi.org/10.1128/EC.00167-06.
57. **Kim SY, Ko YJ, Jung KW, Strain A, Nielsen K, Bahn YS.** 2011. Hrk1 plays both Hog1-dependent and -independent roles in controlling stress response and antifungal drug resistance in Cryptococcus neoformans. PLoS One **6:**e18769. http://dx.doi.org/10.1371/journal.pone.0018769.
58. **Lopez-Aviles S, Grande M, Gonzalez M, Helgesen AL, Alemany V, Sanchez-Piris M, Bachs O, Millar JB, Aligue R.** 2005. Inactivation of the Cdc25 phosphatase by the stress-activated Srk1 kinase in fission yeast. Mol Cell **17:**49–59. http://dx.doi.org/10.1016/j.molcel.2004.11.043.
59. **Di Y, Holmes EJ, Butt A, Dawson K, Mironov A, Kotiadis VN, Gourlay CW, Jones N, Wilkinson CR.** 2012. H_2O_2 stress-specific regulation of S. pombe MAPK StyI by mitochondrial protein phosphatase Ptc4. EMBO J **31:**563–575. http://dx.doi.org/10.1038/emboj.2011.438.
60. **Kashatus JA, Nascimento A, Myers LJ, Sher A, Byrne FL, Hoehn KL, Counter CM, Kashatus DF.** 2015. Erk2 phosphorylation of Drp1 promotes mitochondrial fission and MAPK-driven tumor growth. Mol Cell **57:**537–551. http://dx.doi.org/10.1016/j.molcel.2015.01.002.
61. **Leboucher GP, Tsai YC, Yang M, Shaw KC, Zhou M, Veenstra TD, Glickman MH, Weissman AM.** 2012. Stress-induced phosphorylation and proteasomal degradation of mitofusin 2 facilitates mitochondrial fragmentation and apoptosis. Mol Cell **47:**547–557. http://dx.doi.org/10.1016/j.molcel.2012.05.041.
62. **Reyes G, Romans A, Nguyen CK, May GS.** 2006. Novel mitogen-activated protein kinase MpkC of Aspergillus fumigatus is required for utilization of polyalcohol sugars. Eukaryot Cell **5:**1934–1940. http://dx.doi.org/10.1128/EC.00178-06.
63. **Jun SC, Lee SJ, Park HJ, Kang JY, Leem YE, Yang TH, Chang MH, Kim JM, Jang SH, Kim HG, Han DM, Chae KS, Jahng KY.** 2011. The MpkB MAP kinase plays a role in post-karyogamy processes as well as in hyphal anastomosis during sexual development in Aspergillus nidulans. J Microbiol **49:**418–430. http://dx.doi.org/10.1007/s12275-011-0193-3.
64. **Furukawa K, Hoshi Y, Maeda T, Nakajima T, Abe K.** 2005. Aspergillus nidulans HOG pathway is activated only by two-component signalling pathway in response to osmotic stress. Mol Microbiol **56:**1246–1261. http://dx.doi.org/10.1111/j.1365-2958.2005.04605.x.
65. **Son S, Osmani SA.** 2009. Analysis of all protein phosphatase genes in Aspergillus nidulans identifies a new mitotic regulator, fcp1. Eukaryot Cell **8:**573–585. http://dx.doi.org/10.1128/EC.00346-08.
66. **Blasius M, Wagner SA, Choudhary C, Bartek J, Jackson SP.** 2014. A quantitative 14-3-3 interaction screen connects the nuclear exosome targeting complex to the DNA damage response. Genes Dev **28:**1977–1982. http://dx.doi.org/10.1101/gad.246272.114.
67. **Ye XS, Fincher RR, Tang A, Osmani SA.** 1997. The G_2/M DNA damage checkpoint inhibits mitosis through Tyr15 phosphorylation of p34cdc2 in Aspergillus nidulans. EMBO J **16:**182–192. http://dx.doi.org/10.1093/emboj/16.1.182.
68. **Fernandez-Capetillo O, Lee A, Nussenzweig M, Nussenzweig A.** 2004. H2AX: the histone guardian of the genome. DNA Repair (Amst) **3:**959–967. http://dx.doi.org/10.1016/j.dnarep.2004.03.024.
69. **Swaminathan S, Masek T, Molin C, Pospisek M, Sunnerhagen P.** 2006. Rck2 is required for reprogramming of ribosomes during oxidative stress. Mol Biol Cell **17:**1472–1482. http://dx.doi.org/10.1091/mbc.E05-07-0632.
70. **Ronkina N, Kotlyarov A, Dittrich-Breiholz O, Kracht M, Hitti E, Milarski K, Askew R, Marusic S, Lin LL, Gaestel M, Telliez JB.** 2007. The mitogen-activated protein kinase (MAPK)-activated protein kinases MK2 and MK3 cooperate in stimulation of tumor necrosis factor biosynthesis and stabilization of p38 MAPK. Mol Cell Biol **27:**170–181. http://dx.doi.org/10.1128/MCB.01456-06.
71. **Eisinger-Mathason TS, Andrade J, Groehler AL, Clark DE, Muratore-Schroeder TL, Pasic L, Smith JA, Shabanowitz J, Hunt DF, Macara IG, Lannigan DA.** 2008. Codependent functions of RSK2 and the apoptosis-promoting factor TIA-1 in stress granule assembly and cell survival. Mol Cell **31:**722–736. http://dx.doi.org/10.1016/j.molcel.2008.06.025.
72. **Marhoul JF, Adams TH.** 1996. Aspergillus fabM encodes an essential product that is related to poly(A)-binding proteins and activates development when overexpressed. Genetics **144:**1463–1470.
73. **Dastidar RG, Hooda J, Shah A, Cao TM, Henke RM, Zhang L.** 2012. The nuclear localization of SWI/SNF proteins is subjected to oxygen regulation. Cell Biosci **2:**30. http://dx.doi.org/10.1186/2045-3701-2-30.
74. **Lu J, Kobayashi R, Brill SJ.** 1996. Characterization of a high mobility group 1/2 homolog in yeast. J Biol Chem **271:**33678–33685. http://dx.doi.org/10.1074/jbc.271.52.33678.
75. **Borodkina A, Shatrova A, Abushik P, Nikolsky N, Burova E.** 2014. Interaction between ROS dependent DNA damage, mitochondria and p38 MAPK underlies senescence of human adult stem cells. Aging (Albany NY) **6:**481–495.

76. **Lai CY, Jaruga E, Borghouts C, Jazwinski SM.** 2002. A mutation in the ATP2 gene abrogates the age asymmetry between mother and daughter cells of the yeast Saccharomyces cerevisiae. Genetics **162:**73–87.
77. **Laun P, Pichova A, Madeo F, Fuchs J, Ellinger A, Kohlwein S, Dawes I, Frohlich KU, Breitenbach M.** 2001. Aged mother cells of Saccharomyces cerevisiae show markers of oxidative stress and apoptosis. Mol Microbiol **39:**1166–1173. http://dx.doi.org/10.1111/j.1365-2958.2001.02317.x.
78. **Liao XS, Small WC, Srere PA, Butow RA.** 1991. Intramitochondrial functions regulate nonmitochondrial citrate synthase (CIT2) expression in Saccharomyces cerevisiae. Mol Cell Biol **11:**38–46.
79. **Small WC, Brodeur RD, Sandor A, Fedorova N, Li G, Butow RA, Srere PA.** 1995. Enzymatic and metabolic studies on retrograde regulation mutants of yeast. Biochemistry **34:**5569–5576. http://dx.doi.org/10.1021/bi00016a031.
80. **Ruiz-Roig C, Noriega N, Duch A, Posas F, de Nadal E.** 2012. The Hog1 SAPK controls the Rtg1/Rtg3 transcriptional complex activity by multiple regulatory mechanisms. Mol Biol Cell **23:**4286–4296. http://dx.doi.org/10.1091/mbc.E12-04-0289.
81. **Hynes MJ, Murray SL.** 2010. ATP-citrate lyase is required for production of cytosolic acetyl coenzyme A and development in Aspergillus nidulans. Eukaryot Cell **9:**1039–1048. http://dx.doi.org/10.1128/EC.00080-10.
82. **Lee YJ, Kim KJ, Kang HY, Kim HR, Maeng PJ.** 2012. Involvement of GDH3-encoded NADP+-dependent glutamate dehydrogenase in yeast cell resistance to stress-induced apoptosis in stationary phase cells. J Biol Chem **287:**44221–44233. http://dx.doi.org/10.1074/jbc.M112.375360.
83. **Shiozaki K, Russell P.** 1996. Conjugation, meiosis, and the osmotic stress response are regulated by Spc1 kinase through Atf1 transcription factor in fission yeast. Genes Dev **10:**2276–2288. http://dx.doi.org/10.1101/gad.10.18.2276.
84. **Machida K, Tanaka T, Fujita K, Taniguchi M.** 1998. Farnesol-induced generation of reactive oxygen species via indirect inhibition of the mitochondrial electron transport chain in the yeast Saccharomyces cerevisiae. J Bacteriol **180:**4460–4465.
85. **Semighini CP, Hornby JM, Dumitru R, Nickerson KW, Harris SD.** 2006. Farnesol-induced apoptosis in Aspergillus nidulans reveals a possible mechanism for antagonistic interactions between fungi. Mol Microbiol **59:**753–764. http://dx.doi.org/10.1111/j.1365-2958.2005.04976.x.
86. **Dichtl K, Ebel F, Dirr F, Routier FH, Heesemann J, Wagener J.** 2010. Farnesol misplaces tip-localized Rho proteins and inhibits cell wall integrity signalling in Aspergillus fumigatus. Mol Microbiol **76:**1191–1204. http://dx.doi.org/10.1111/j.1365-2958.2010.07170.x.
87. **Machida K, Tanaka T, Yano Y, Otani S, Taniguchi M.** 1999. Farnesol-induced growth inhibition in Saccharomyces cerevisiae by a cell cycle mechanism. Microbiology **145:**293–299. http://dx.doi.org/10.1099/13500872-145-2-293.